Chapter 3: Materials and methods

The materials and methods used within this study area are given, as are the standardised units and keys used in the sediment descriptions.

3.1 OSL sampling

Samples for OSL dating were collected using a Geoprobe coring rig (Fig. 3.1). After an area was selected that for dating, e.g. a block of terrace, a series of thin gouge cores were recorded to interpret the stratigraphy of the terrace and assess the basal sand unit for sample collection. If a basal sand lense of 20cm or greater was encountered then sample collection proceeded.

The Geoprobe was driven around the study area in a trailer hitched to a Landrover; meaning vehicular access was required to any sample location. The Geoprobe uses a closed chamber to collect sample cores. The chamber is 1.22m in length, with a plastic tube held inside that is 3cm in diameter (Fig. 3.2). The plastic tubes were made opaque through numerous coats of black paint applied to their exterior. A metal cutter is attached to the bottom of the collection chamber and the core is inserted into the ground. As much of the sampling as possible was done through pressure driving to minimise sample disturbance. However, hammer (percussion) drives had to be used in specific instance to get through high resistance sediment units.

Once the stratigraphy of the sample area had been ascertained a tube collected a depth to c. 25cm into the gravel body; e.g. if a 2.22m sequence to gravels was recorded the first 1.22m would be sample and discarded. A collection tube would then be inserted into the closed chamber and a second drive of 1.22m – 2.44m would be collected. This would allow the basal sands to be sampled in the tube and be capped by 22cm of gravel. The stratigraphy and depth to the basal sands was carefully noted on each sample tube. The ends were stopped and the tube was wrapped in silver foil to stop any post sampling light contamination.

3.1.1 Optical dating: Mechanisms and principles

Upon exposure to ionising radiation, electrons within the crystal lattice of insulating minerals are displaced from their atomic orbits. Whilst this dislocation is momentary for most electrons, a portion of charge is redistributed to meta-stable sites (traps) within the crystal lattice. In the absence of significant optical and thermal stimuli, this charge can be stored for extensive periods. The quantity of charge relocation and storage relates to the magnitude and period of irradiation. When the lattice is optically or thermally stimulated, charge is evicted from traps and may return to a vacant orbit position (hole). Upon recombination with a hole, an electron's energy can be dissipated in the form of light generating crystal luminescence providing a measure of dose absorption.

In this study quartz was segregated for dating. The utility of this minerogenic dosimeter lies in the stability of its datable signal over the mid to late Quaternary period, predicted through isothermal decay studies (e.g. Smith *et al.,* 1990; retention lifetime 630 Ma at 20°C) and evidenced by optical age estimates concordant with independent chronological controls (e.g. Murray and Olley, 2002) This stability is in contrast to the anomalous fading of comparable

signals commonly observed for other ubiquitous sedimentary minerals such as feldspar and zircon (Wintle, 1973; Templer, 1985; Spooner, 1993).

Optical age estimates of sedimentation (Huntley *et al.*, 1985) are premised upon reduction of the minerogenic time dependent signal (Optically Stimulated Luminescence, OSL) to zero through exposure to sunlight and, once buried, signal reformulation by absorption of litho- and cosmogenic radiation. The signal accumulated post burial acts as a dosimeter recording total dose absorption, converting to a chronometer by estimating the rate of dose absorption quantified through the assay of radioactivity in the surrounding lithology and streaming from the cosmos.

$$\text{Age} = \frac{\text{Mean Equivalent Dose } (D_e, \text{Gy})}{\text{Mean Dose Rate } (D_r, \text{Gy.ka}^{-1})}$$

Aitken (1998) and Bøtter-Jensen et al. (2003) offer a detailed review of optical dating.

3.1.2 Sample Collection and Preparation

Twenty one conventional sediment samples – those located within matrix-supported units composed predominantly of sand and silt - were collected within opaque plastic tubing from either sections by means of tubing (150x45 mm) forced into each face (samples GL06005 to GL06009) or from boreholes excavated by a Geoprobe (in tubing 1000x45 mm). Each sample location marked the deepest points of palaeochannels within the study area. Each tube was wrapped in cellophane and parcel tape in order to preserve moisture content and integrity until ready for laboratory preparation. To preclude optical erosion of the datable signal prior to measurement, all samples were prepared under controlled laboratory illumination provided by Encapsulite RB-10 (red) filters. To isolate that material potentially exposed to daylight during sampling or that which had been relocated by the process of coring, sediment located within the outer 5 mm of each sample was removed.

The remaining sample was dried and then sieved. Quartz within the fine sand (125-180 μm or 180-250 μm) fraction was then segregated. Samples were subjected to acid and alkali digestion (10% HCl, 15% H_2O_2) to attain removal of carbonate and organic components respectively.

A further acid digestion in HF (40%, 60 minutes) was used to etch the outer 10-15 μm layer affected by α radiation and degrade each samples' feldspar content. During HF treatment, continuous magnetic stirring was used to effect isotropic etching of grains. 10% HCl was then added to remove acid soluble fluorides. Each sample was dried, resieved and quartz isolated from the remaining heavy mineral fraction using a sodium polytungstate density separation at 2.68g.cm^{-3}. Where sufficient datable mass existed, 24 multi-grain aliquots (c. 3-6 mg) of quartz from each sample were then mounted on aluminium discs to establish optimum, average measurement conditions for single grain aliquots. Around 2400 sand grains from each sample were located individually in 200 mm (diameter and depth) holes drilled as a 10x10 grid into anodised aluminium discs (Duller *et al.*, 1999) to gain a measure of inter-grain D_e distribution.

All drying was conducted at 40°C to prevent thermal erosion of the signal. All acids and alkalis were Analar grade. All dilutions (removing toxic-corrosive and non-minerogenic,

luminescence-bearing substances) were conducted with distilled water to prevent signal contamination by extraneous particles.

3.1.3 Acquisition and accuracy of D_e value

All minerals naturally exhibit marked inter-sample variability in luminescence per unit dose (sensitivity). Therefore, the estimation of D_e acquired since burial requires calibration of the natural signal using known amounts of laboratory dose. D_e values were quantified using a single-aliquot regenerative-dose (SAR) protocol (Murray and Wintle 2000; 2003) facilitated by a Risø TL-DA-15 irradiation-stimulation-detection system (Markey *et al.*, 1997; Bøtter-Jensen et al., 1999; Duller et al., 1999). Within this apparatus, optical signal stimulation of multi-grain aliquots was provided by an assembly of blue diodes (5 packs of 6 Nichia NSPB500S), filtered to 470±80 nm conveying 15 $mW.cm^{-2}$ using a 3 mm Schott GG420 positioned in front of each diode pack. Optical stimulation of single grain aliquots emanated from a focussed solid state 532 nm (green), 10 mW stabilised laser (Laser 2000 LCL-LCM-T-11ccs) scanned across grains by means of mirrors mounted on and moved by motorised linear stages. Infrared (IR) stimulation, provided by 6 IR diodes (Telefunken TSHA 6203) stimulating at 875±80nm delivering ~5 $mW.cm^{-2}$, was used to indicate the presence of contaminant feldspars (Duller, 2003). Stimulated photon emissions from quartz aliquots are in the ultraviolet (UV) range and were filtered from stimulating photons by 7.5 mm HOYA U-340 glass and detected by an EMI 9235QA photomultiplier fitted with a blue-green sensitive bialkali photocathode. Aliquot irradiation was conducted using a 1.48 GBq $^{90}Sr/^{90}Y$ β source calibrated for single and multi-grain aliquots of each isolated quartz fraction against the 'Hotspot 800' ^{60}Co γ source located at the National Physical Laboratory (NPL), UK. In calibrating single sand grain aliquots, no significant spatial variation in dose rate from the β source was found.

SAR by definition evaluates D_e through measuring the natural signal of a single aliquot and then regenerating that aliquot's signal by using known laboratory doses to enable calibration. For each aliquot, at least 4 different regenerative-doses were administered so as to image dose response. D_e values for each aliquot were then interpolated, and associated counting and fitting errors calculated, by way of exponential or exponential plus linear regression. The accuracy with which D_e equates to total absorbed dose and that dose absorbed since burial is assessed. The former can be considered a function of laboratory factors, the latter, one of environmental issues. Diagnostics were deployed to estimate the influence of these factors and criteria instituted to optimise the accuracy of D_e values.

3.1.4 Laboratory Factors

3.1.4.1 Feldspar contamination

The propensity of feldspar signals to fade and underestimate age, coupled with their higher sensitivity relative to quartz makes it imperative to quantify feldspar contamination. At room temperature, feldspars generate a signal (IRSL) upon exposure to IR whereas quartz does not. The signal from feldspars contributing to OSL can be depleted by prior exposure to IR. For all aliquots the contribution of any remaining feldspars was estimated from the OSL IR depletion ratio (Duller, 2003). If the addition to OSL by feldspars is insignificant, then the

repeat dose ratio of OSL to post-IR OSL should be statistically consistent with unity. Any aliquots that did not fulfil this criterion were rejected.

3.1.4.2 Preheating

Preheating aliquots between irradiation and optical stimulation is necessary to ensure comparability between natural and laboratory-induced signals. However, the multiple irradiation and preheating steps that are required to define single-aliquot regenerative-dose response leads to signal sensitisation, rendering calibration of the natural signal inaccurate. The SAR protocol (Murray and Wintle, 2000; 2003) enables this sensitisation to be monitored and corrected using a test dose, here set at c 5 Gy preheated to 220°C for 10s, to track signal sensitivity between irradiation-preheat steps. However, the accuracy of sensitisation correction for both natural and laboratory signals can be preheat dependent. Three diagnostics were used to assess the optimal preheat temperature for accurate correction and calibration.

Irradiation-preheat cycling quantifies the preheat dependence of sensitisation correction for laboratory-induced signals. If sensitisation is accurately corrected, then the same regenerative-dose should yield an equivalent sensitivity corrected value irrespective of the number of times it is applied and its associated signal measured. The ratio of subsequent to initial corrected regenerative-dose signals should be statistically concordant with unity. Alternatively, this ratio may differ from unity yet attain consistency after one or more cycles evidencing accurate sensitivity correction exists if the sample is primed by irradiation-preheat cycles. For this diagnostic, and where sufficient material was available, 18 multi-grain aliquots were divided into sets of 3 and assigned a 10 s preheat between 180°C and 280°C.

D_e preheat dependence quantifies the combined effects of thermal transfer and sensitisation on the natural signal. Insignificant adjustment in D_e values in response to differing preheats may reflect limited influence of these effects. Samples generating D_e values <10Gy and exhibiting a systematic, statistically significant adjustment in D_e value with increasing preheat temperature may indicate the presence of significant thermal transfer; in such instances low temperature (<220°C) preheats may provide the apposite measure of D_e. For this diagnostic, the D_e value of each of the same 18 multi-grain aliquots and their assigned preheat was assessed.

Dose Recovery attempts to replicate the above diagnostic, yet provide improved resolution of thermal effects through removal of variability induced by heterogeneous dose absorption in the environment, using a precise laboratory dose to simulate natural dose. The ratio between the applied dose and recovered D_e value should be statistically concordant with unity. For this diagnostic, a further 6 multi-grain aliquots were each assigned a 10 s preheat between 180°C and 280°C.

That preheat treatment fulfilling the criterion of accuracy for all three diagnostics was selected to refine the final D_e value for 2400 single grain aliquots. Further thermal treatments, prescribed by Murray and Wintle (2000; 2003), were applied to optimise accuracy and precision. Optical stimulation occurred at 125ºC in order to minimise effects associated with photo-transferred thermoluminescence and maximise signal to noise ratios. Inter-cycle optical stimulation was conducted at 280°C to minimise recuperation.

3.4.1.3 Irradiation

Laboratory irradiation effects may evolve from the contrasting rates of natural dose exposure and the calibrating laboratory dose, the latter delivered to each aliquot at 9 orders of magnitude faster than the former. Bailey (2004) has suggested that for doses in excess of ~40 Gy an overestimation of age may arise due to competing mechanisms of signal accumulation within the crystal lattice of quartz. Only one sample (GL06009) generated single grain D_e values >40 Gy. These accounted for the minority of D_e values obtained for GL06009 and therefore laboratory irradiation effects were not considered significant in this study.

3.1.4.3 Internal consistency

Radial plots (Fig. 5; cf Galbraith, 1990) are used to illustrate inter-aliquot D_e variability for natural and regenerated signals. D_e values are standardised relative to the central D_e value (Galbraith *et al.*, 1999) for natural signals and applied dose for regenerated signals. D_e values are described as over dispersed when >5% lie beyond $\pm$ 2σ of the standardising value; resulting from a heterogeneous absorption of burial dose and/or response to the SAR protocol. Over dispersion for natural signals does not necessarily imply inaccuracy. However where over dispersion is observed for regenerated signals, the age estimate from that sample should be accepted tentatively.

3.1.5 Environmental factors

3.1.5.1 Incomplete zeroing

Post-burial OSL signals residual of pre-burial dose absorption can result where pre-burial sunlight exposure is limited in spectrum, intensity and/or period, leading to age overestimation. This effect is particularly acute for material eroded and redeposited sub-aqueously (Olley *et al*., 1998, 1999; Wallinga, 2002) and exposed to a burial dose of <20 Gy (e.g. Olley *et al.*, 2004). It can have some influence in sub-aerial contexts but is rarely of consequence where aerial transport has occurred. Optical dating of dominantly Holocene fluvial sands within this study warrants that this environmental effect be addressed.

Within single-aliquot regenerative-dose optical dating there are two diagnostics of partial resetting (or bleaching); signal analysis (Agersnap-Larsen et al., 2000; Bailey et al., 2003) and inter-aliquot D_e distribution studies (Murray et al., 1995).

Within this study the latter has been used, taking aliquots of single sand grains to quantify inter-grain D_e distribution. At present, it is contended that asymmetric inter-grain D_e distributions are symptomatic of partial bleaching and/or pedoturbation (Murray et al., 1995; Olley et al., 1999; Olley et al., 2004; Bateman et al., 2003). For partial bleaching at least, it is further contended that the D_e acquired during burial is located in the minimum region of such ranges. The Minimum Age Model (Galbraith and Laslett, 1993) is the most regularly applied statistical approach in quantifying the breadth of minimum dose regions. Olley et al. (2004) recommend this model for Holocene fluvial samples based upon its agreement with independent age controls for a number of samples. Yet such models have been found to underestimate post-burial D_e values owing to post depositional turbation (Roberts et al.,

1998) or as a product of a minority of outlying low D_e values (Rodnight, 2006). The Finite Mixture Model (Galbraith and Green, 1990) offers an alternative statistical method by which to compute the minimum dose region reflecting post-burial D_e. It identifies the number of dose components within an inter-grain D_e distribution along with the mean D_e and proportion of grains in each component. In the Finite Mixture Model each component is assumed to have an equivalent level of over dispersion (σ, herein set at 0.10; Jacobs et al., 2006; Rodnight et al., 2006). Rodnight et al. (2006) advocate use of the youngest component unless it comprises less than 10% of aliquots, whereupon the next youngest component is taken to reflect post-burial D_e. However, the mean and breadth of this minimum region in all models is the subject of current debate, as it is additionally influenced by heterogeneity in microdosimetry, variable inter-grain response to SAR and residual to post-burial signal ratios. The Central Age Model (Galbraith et al., 1999) assumes all inter-grain D_e variation is forced by spatial variations in dose rate and natural irradiation effects that can be accurately replicated by laboratory irradiation, and thus the mean D_e value coupled with the mean D_r value will generate an accurate age estimate of burial. At present, it is clear that age defined by the D_e interval delimited by the Minimum and Central Age Models will be accurate but have limited precision (Table 1). In this study, the Finite Mixture Model has been adopted to produce a more refined estimate of age (Table 1) based on the success of its implementation by Rodnight et al. (2006) in sediments equivalent in age and genus to those in this study.

3.1.5.2 Turbation

The accuracy of sedimentation ages can further be controlled by post-burial trans-strata grain movements forced by pedo- or cryoturbation. Berger (2003) contends pedogenesis prompts a reduction in the apparent sedimentation age of parent material through bioturbation and illuviation of younger material from above and/or by biological recycling and resetting of the datable signal of surface material. Berger (2003) proposes that the chronological products of this remobilisation are A-horizon age estimates reflecting the cessation of pedogenic activity, Bc/C-horizon ages delimiting the maximum age for the initiation of pedogenesis with estimates obtained from Bt-horizons providing an intermediate age 'close to the age of cessation of soil development'. Singhvi et al. (2001), in contrast, suggest that B and C-horizons closely approximate the age of the parent material, the A-horizon, that of the 'soil forming episode'. At present there is no post-sampling mechanism for the direct detection of and correction for post-burial sediment remobilisation. However, intervals of palaeosol evolution can be delimited by a maximum age derived from parent material and a minimum age obtained from a unit overlying the palaeosol. Pedogenic effects are not considered significant within this study owing to the lack of visible soil development. Inaccuracy forced by cryoturbation may be bidirectional, heaving older material upwards or drawing younger material downwards into the level to be dated. However, only one sample (GL06009) was retrieved from a section of sediments likely dating to the last glacial stage; no evidence was observed of cryogenic deformation.

3.1.6 Acquisition and accuracy of D_r value

Lithogenic D_r values were defined through measurement of U, Th and K radionuclide concentration and conversion of these quantities into β and γ D_r values. β contributions were estimated from sub-samples by Neutron Activation Analysis (NAA) delivered by Becquerel

Canada. γ dose rates were estimated for samples GL06005 to GL06009 from in situ NaI γ spectrometry. Where direct measurements of γ dose rate were not possible, laboratory-based Ge γ spectrometry was conducted on sub-samples composed of material at intervals within 300 mm above and below the centre of each sample within each core (weighted by relative γ contributions; Aitken, 1985). In situ measurements were conducted using an EG&G μNomad portable NaI γ spectrometer (calibrated using the block standards at RLAHA, University of Oxford); these reduce uncertainty relating to potential heterogeneity in the γ dose field surrounding each sample. Laboratory-based γ spectrometry was conducted using an Ortec GEM-S high purity Ge coaxial detector system, calibrated using certified reference materials supplied by CANMET. Estimates of radionuclide concentration were converted into D_r values (Adamiec and Aitken, 1998), accounting for D_r modulation forced by grain size (Mejdahl, 1979) and present moisture content (Zimmerman, 1971). Cosmogenic D_r values are calculated on the basis of sample depth, geographical position and matrix density (Prescott and Hutton, 1994).

The spatiotemporal validity of D_r values can be considered as a function of five variables. Firstly, age estimates devoid of in situ γ spectrometry data should be accepted tentatively if the sampled unit is heterogeneous in texture or if the sample is located within 300 mm of strata consisting of differing texture and/or mineralogy. However, where samples are obtained throughout a vertical profile, consistent values of γ D_r based solely on, for example, NAA may evidence the homogeneity of the γ field and hence accuracy of γ D_r values. Secondly, disequilibrium can force temporal instability in U and Th emissions. In this study, the potential for long-term instability in D_r values forced by U disequilibrium has been considered. The impact of this infrequent phenomenon (Olley et al., 1996) upon age estimates is usually insignificant given their associated margins of error, however this effect is pronounced for at least two samples in this study (>50% disequilibrium between ^{238}U and ^{226}Ra, samples GL06014 & GL06025). Thirdly, pedogenically-induced variations in matrix composition of B and C-horizons, such as radionuclide and/or mineral remobilisation, may alter the rate of energy emission and/or absorption. If D_r is invariant through a dated profile and samples encompass primary parent material, then element mobility is likely limited in effect. In this study, there is limited evidence of pedogenesis in any unit sampled. Fourthly, spatiotemporal deviations from present moisture content are difficult to assess directly, requiring knowledge of the magnitude and timing of differing contents. However, the maximum influence of moisture content variations can be delimited by recalculating D_r for minimum (zero) and maximum (saturation) content. Finally, temporal alteration in the thickness of overburden alters cosmic D_r values. Cosmic D_r often forms a negligible portion of total D_r. It is possible to quantify the maximum influence of overburden flux by recalculating D_r for minimum (zero) and maximum (surface sample) cosmic D_r.

3.1.7 Estimation of Age

Age estimates provide an estimate of sediment burial period based on mean D_r values and D_e values derived from Minimum, Finite Mixture and Central Age Models, along with associated analytical uncertainties. Uncertainty in Finite Mixture age estimates is reported as a product of systematic and experimental errors, with the magnitude of experimental errors alone shown in parenthesis. Probability distributions indicate the inter-aliquot variability in age. The maximum influence of temporal variations in D_r forced by minima-maxima variation in moisture content and overburden thickness, coupled with Finite Mixture D_e

values. Where uncertainty in these parameters exists this age range may prove instructive, however the combined extremes represented should not be construed as preferred age estimates.

3.1.8 Analytical uncertainty

All errors are based upon analytical uncertainty and quoted at 1σ confidence. Error calculations account for the propagation of systematic and/or experimental (random) errors associated with D_e and D_r values.

For D_e values, systematic errors are confined to laboratory β source calibration. Uncertainty in this respect is that combined from the delivery of the calibrating γ dose (1.2%; NPL, pers. comm.), the conversion of this dose for SiO_2 using the respective mass energy-absorption coefficient (2%; Hubbell, 1982), reproducibility in laser positioning (3.5%; Truscott *et al.*, 2000) and experimental error, totalling 4.3%. Mass attenuation and bremsstrahlung losses during γ dose delivery are considered negligible. Experimental errors relate to D_e interpolation using sensitisation corrected dose responses. Natural and regenerated sensitisation corrected dose points (S_i) are quantified by,

$$S_i = (D_i - x.L_i) / (d_i - x.L_i) \quad \text{Eq.1}$$

where D_i = Natural or regenerated OSL, initial 0.2 s
L_i = Background natural or regenerated OSL, final 5 s
d_i = Test dose OSL, initial 0.2 s
x = Scaling factor, 0.08

The error on each signal parameter is based on counting statistics, reflected by the square-root of measured values. The propagation of these errors within Eq. 1 generating σS_i follows the general formula given in Eq. 2. σS_i are then used to define fitting and interpolation errors within linear or exponential regressions (Green and Margerison, 1978; Ixaru et al., 2004).

For D_r values, systematic errors accommodate uncertainty in radionuclide conversion factors (5%), β attenuation coefficients (5%), matrix density (0.20 $g.cm^{-3}$), vertical thickness of sampled section (specific to sample collection device), saturation moisture content (3%), moisture content attenuation (2%), burial moisture content (25% relative, unless direct evidence exists of the magnitude and period of differing content), NaI gamma spectrometer calibration (3%) and/or NAA (2%). Experimental errors are associated with radionuclide quantification for each sample by γ spectrometry and/or NAA.

The propagation of these errors through to age calculation is quantified using the expression,

$$\sigma y\,(\delta y/\delta x) = (\Sigma\,((\delta y/\delta x_n).\sigma x_n)^2)^{1/2} \quad \text{Eq. 2}$$

where y is a value equivalent to that function comprising terms x_n and where σy and σx_n are associated uncertainties.

Errors on age estimates based on the Finite Mixture Model are presented as combined systematic and experimental errors and experimental errors alone. The former (combined) error should be considered when comparing luminescence ages herein with independent chronometric controls. The latter assumes systematic errors are common to luminescence age estimates generated by means equal to those detailed herein and enable direct comparison with those estimates.

3.1.9 Intrinsic Assessment of Reliability

In this study, intrinsic assessment of reliability is restricted to analytical acceptability. Other indexes of reliability in Optical dating can be drawn by inference. Intra-site stratigraphic consistency of ages, quantified by Bayesian modelling, and the convergence of age estimates from stratigraphically equivalent units of divergent dosimetry are key intrinsic measures of reliability (Toms *et al*., 2005). However, the low sampling density per dated level and ambiguity in inter-core relative stratigraphic position of samples precluded the use of these inferential methods.

Fig 3.1: The Geoprobe coring rig, about to commence a drive. The closed metal chamber is seen at the front of the rig, with a plastic sample collection tube located within it.

Fig 3.2: A sample recovered from the Geoprobe. The sample collection tube is shown coming out of the closed metal sampling chamber. The sample collection tubes used for OSL sampling were black opaque tubes.

3.2 Radiocarbon and pollen sample collection

A series of palaeochannels across the study area were selected for pollen sample collection and associated radiocarbon dating. Two strategies were employed to retrieve these samples: tin collection (Warren Farm Quarry) and gouge core collection (general study area). The location of all samples was recorded using differential GPS. The location of all the sample locations is given (Fig. 3.3).

3.2.1 Tin collection Warren Farm Quarry

The opportunity to record the exposed sections in Warren Farm Quarry, allowed a series of targeted samples to be collected. The location of the recorded sections and palaeochannels is given for the quarry (Fig. 3.4). The associated section drawings are also given, along with a photograph of each palaeochannel sampled (Fig 3.5 and 3.6).

Sampling used 50cm long, 10cm deep collection tins that were hammered into the sections. The tins were prized away form the section using a spade and immediately wrapped with cling film (to prevent water loss) and silver foil. The orientation and sample number was recorded on each tin. In total four palaeochannels within the quarry were selected for pollen assessment and are summarised as:

WFQ C1: 3 tins were recovered from the exposed palaeochannel, giving a total sample depth of 124cm (Figs 3.5 and 3.7).

WFQ C2: 3 tins were recovered from the exposed palaeochannel, giving a total sample depth of 1.23m (Figs. 3.5 and 3.8).

WFQ C3: 1 tin was recovered from the exposed palaeochannel, giving a sample depth of 50cm (Figs. 3.6 and 3.7).

WFQ C5: 1 tin was recovered from the exposed palaeochannel, giving a sample depth of 50cm (Fig. 3.6).

'Bulk samples collected for Coleopteran evaluation were adjacent to the tin samples collected for pollen. Thus a depth of WQFC5 10cm, is the same for both pollen and Coleopteran evaluations'.

3.2.2 Gouge core sampling

A series of palaeochannels were sampled across the general study area for pollen. Assessment of suitable sampling locations had to be made using LiDAR, after the GPR proved ineffective at penetrating palaeochannel fills (Phase 1). Palaeochannels were initially cored using a thin 2cm gouge, to assess the sediment stratigraphy. After assessment either the section of palaeochannel was abandoned or sample collection proceeded using an 8cm diameter gouge core. Retrieved samples were wrapped in cling film and placed in plastic guttering lengths of 1m each. Sample labels and depths were recorded on each gutter before wrapping in silver foil.

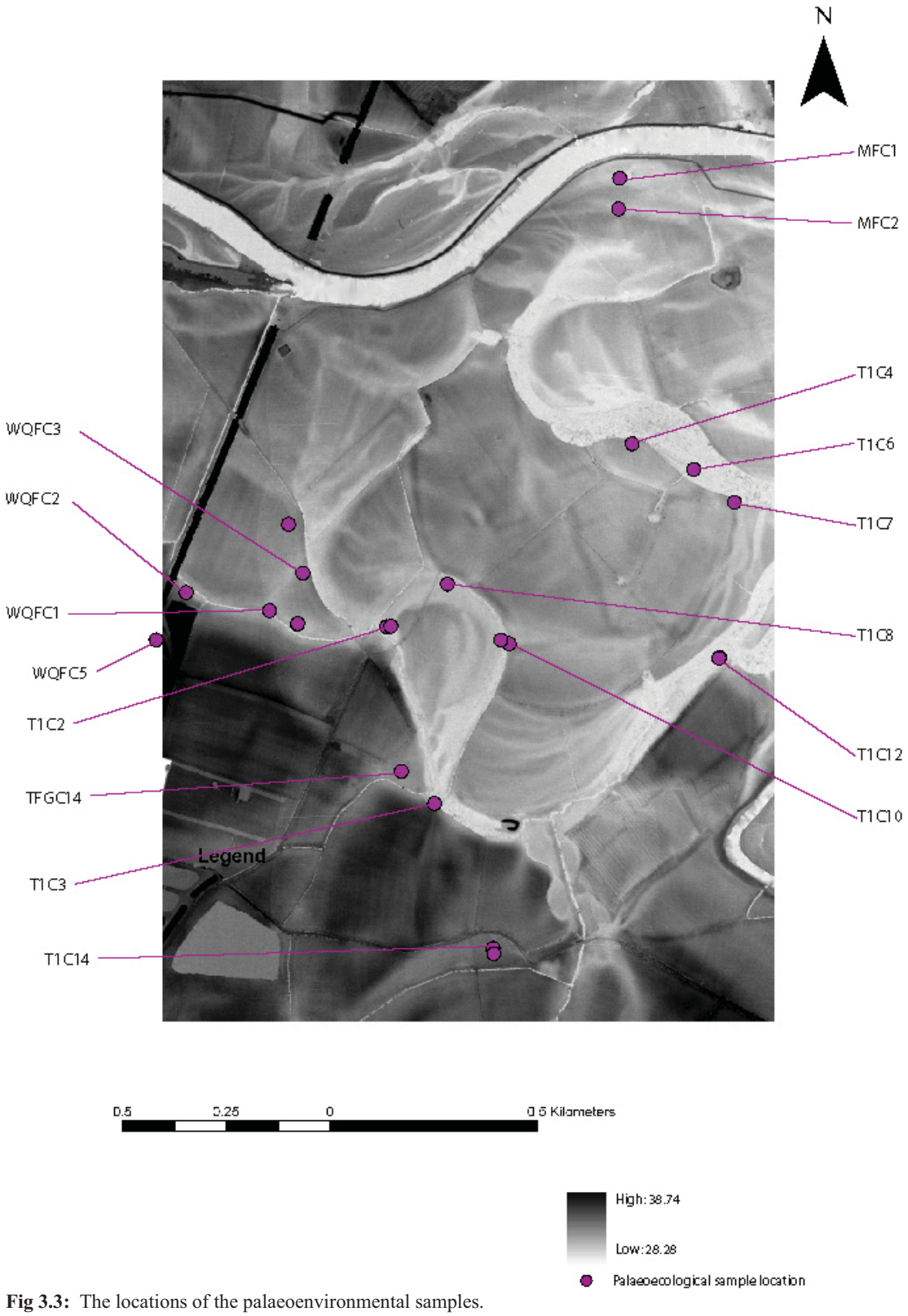

Fig 3.3: The locations of the palaeoenvironmental samples.

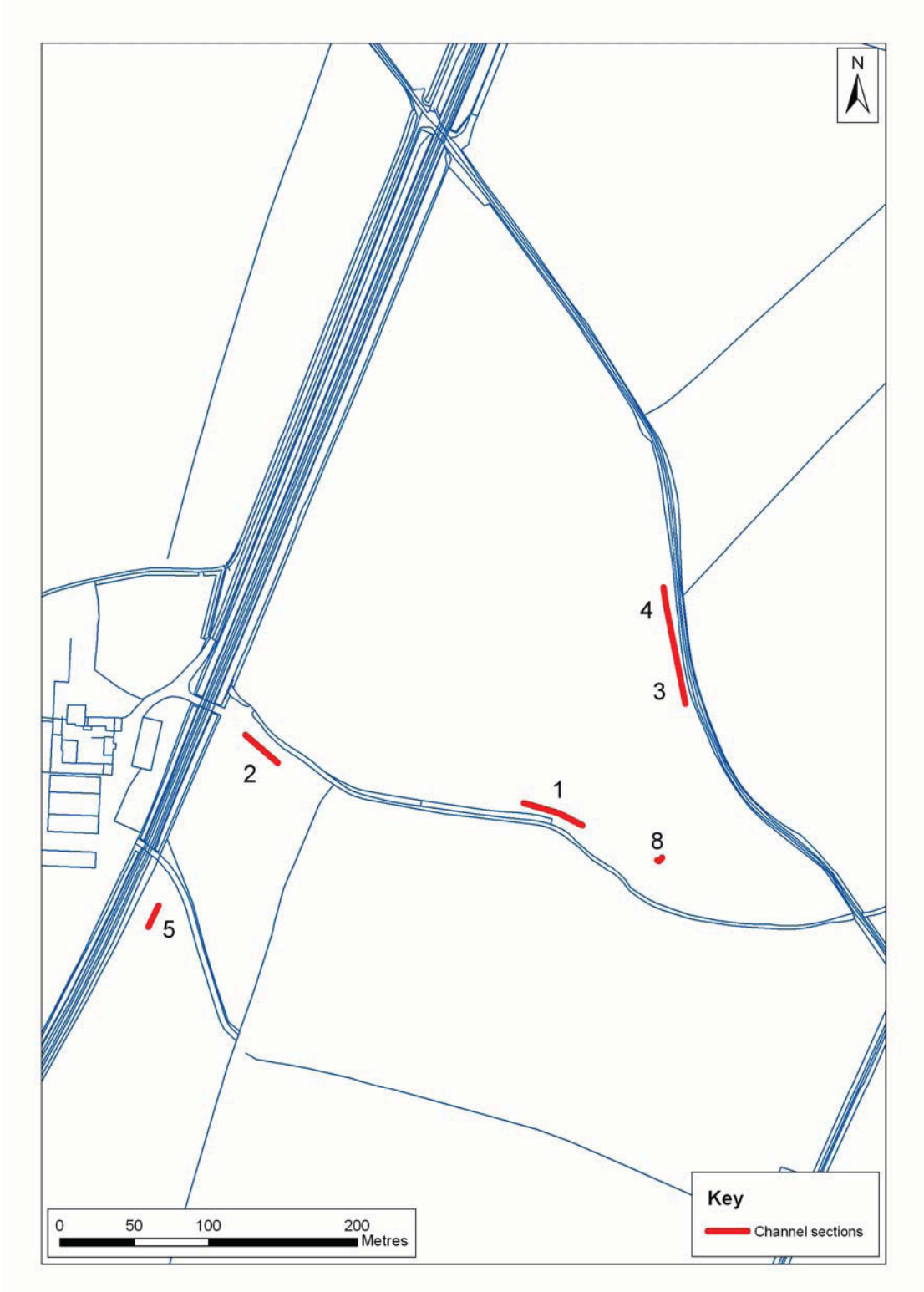

Fig 3.4: The location of the palaeochannels sampled in the quarry and the exposed section that were drawn.

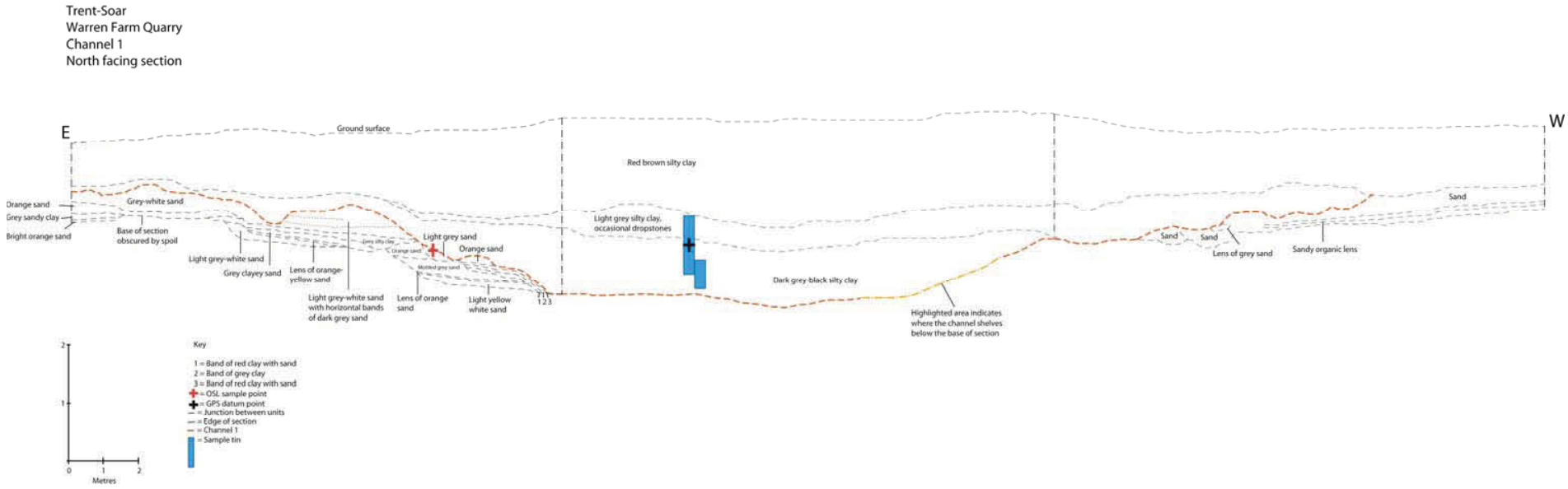

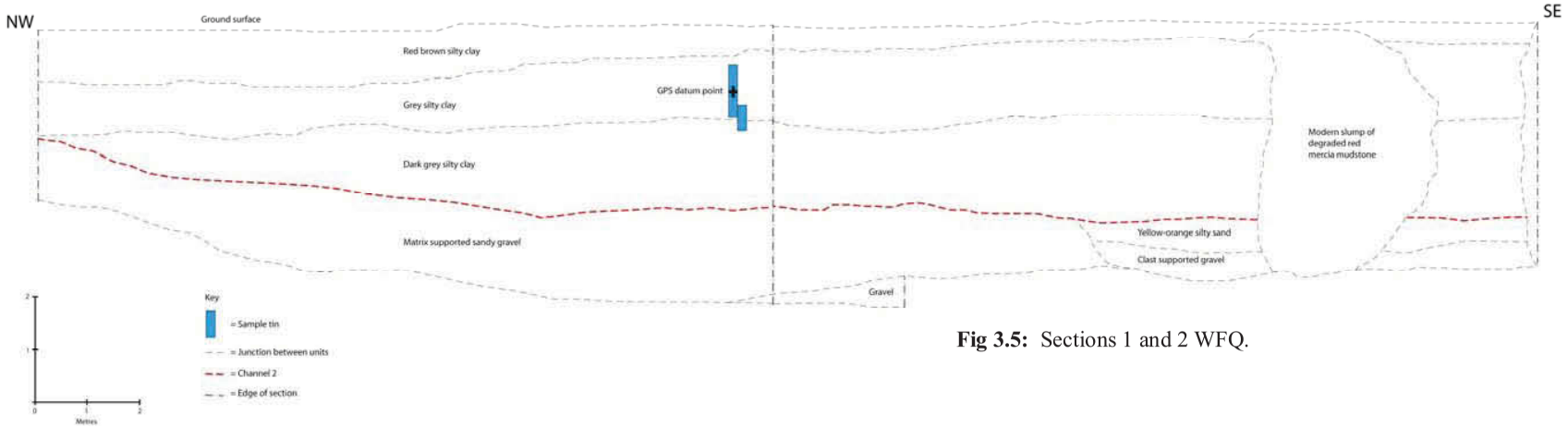

Fig 3.5: Sections 1 and 2 WFQ.

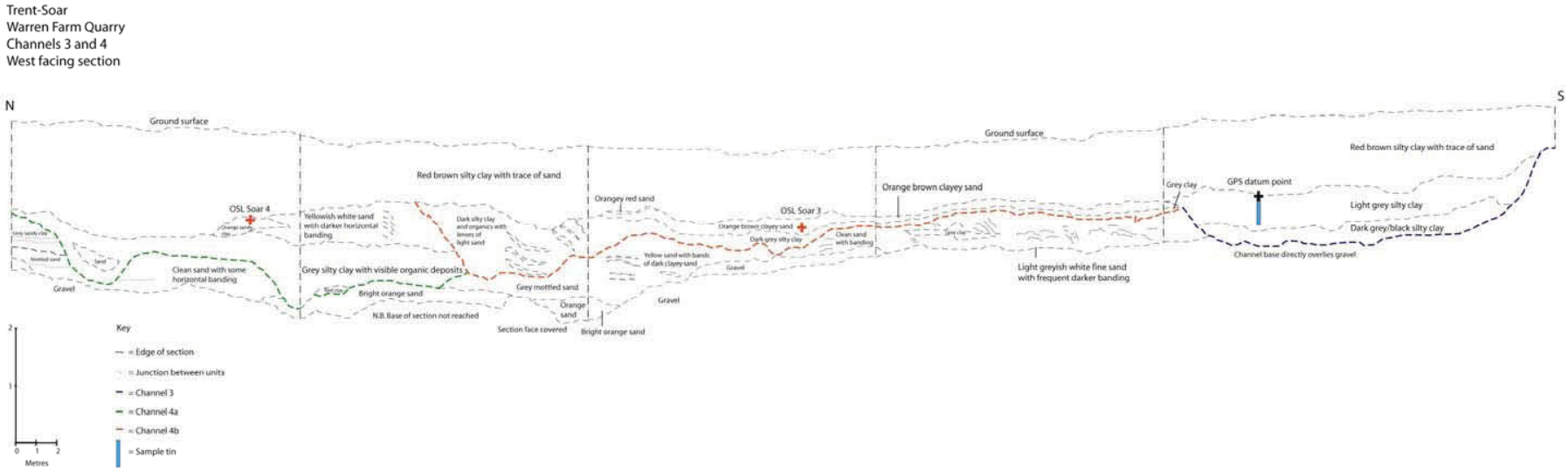

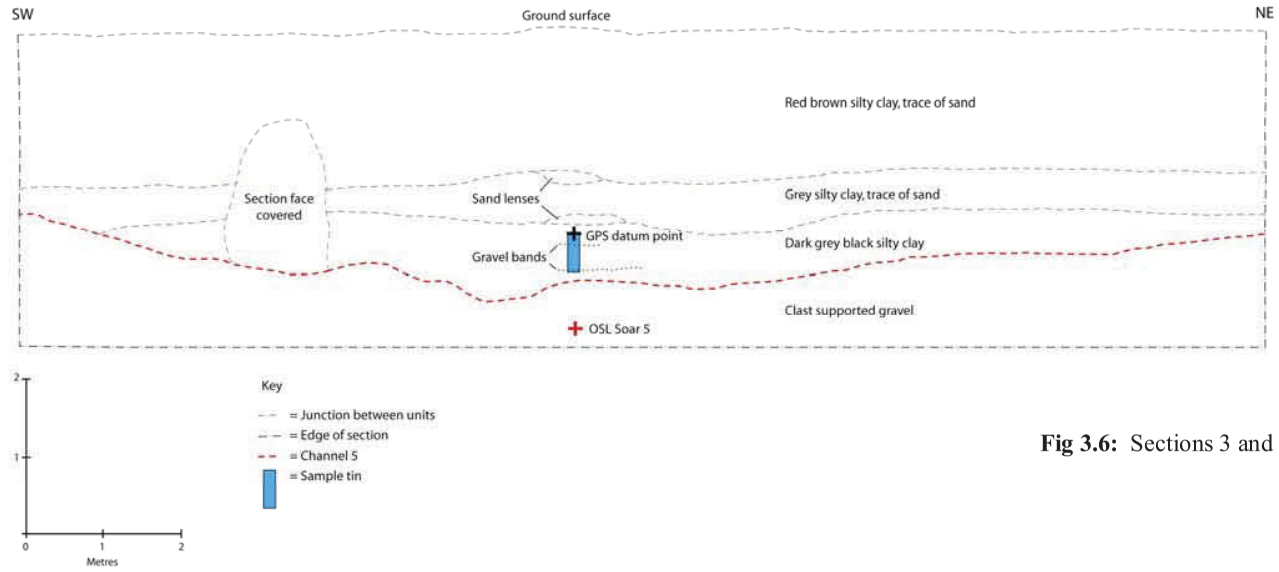

Fig 3.6: Sections 3 and 4 WFQ.

Fig 3.7: Palaeochannel WFQ C1 during sampling.

Fig 3.7: Palaeochannel WFQ C2 during sampling, with the tins *in-situ* before removal. The stratigraphy drawn in the section of red-brown silty clay above a grey silty clay, above a dark grey silty clay is clearly visible.

Fig 3.8: Palaeochannel WQFC3.

3.2.3 Pollen sample methods

Once back in the laboratory the cores and tins were cleaned back, removing material from their outer surfaces. All of the tins and specific cores were selected for detailed analysis. Pollen samples were collected at 14cm intervals, removed from the core/tin using a clean scalpel and spatula. The samples were placed in plastic bags in cold storage for sample digestion. Pollen and spore extraction used the standard chemical processing method using hydrofluoric acid digestion followed by acetolysis (Moore *et al.* 1991). Triple sieving was employed using 200µm and 70µm sieves. A standard volume was used of 1 ml of sediment. This chemical method was preferred over differential density separation (Takeshi 1998) as it is the most commonly used method and provides a standard reference with most published studies. Pollen concentrations were determined by the addition of *Lycopodium clavatum* tablets containing a known number of spores (Stockmarr, 1971). Pollen identification routinely used x 400 magnification with x 1000 magnification for small and difficult types with reference to standard keys (Andrew, 1984; Faegri and Iversen, 1989; Moore et al., 1991) and the Exeter University Pollen and Spore reference collection. Pollen and spore nomenclature follows Bennett *et al.* (1994).

3.2.4 Radiocarbon sample methods

The collection of radiocarbon samples aimed to provide a basal date on all cores and tins. Cores and tins selected for pollen analysis had additional samples removed for radiocarbon dating at 50cm intervals. The removed sediment was placed in a 2mm

stainless steel sieve. Hot water was run over the sample to break up the soil matrix (mainly clay particulates) and reveal the organic matter. Organic samples were removed from the sieve using tweezers and placed in distilled water. This organic component was viewed under a light microscope to look at the integrity of the samples, for factors such as evidence of rolling, whether the sample is a rootlet that had penetrated from higher levels, etc, and for a basic identification. The best elements of the organic fraction were selected for dating and dried for several days at 50^{O}C. A dry weight was then measured on this component. In cases where a sample did not provide sufficient organic material a second sample was selected. If this again failed to produce an organic component of sufficient quality a bulk sediment sample was used for RC dating.

A total of 37 samples were submitted for radiocarbon dating by Accelerator Mass Spectrometry (AMS), producing a total of 39 results, to the Oxford Radiocarbon Accelerator Unit (ORAU) and the Centre for Isotope Study, the University of Groningen, The Netherlands. These consisted of two waterlogged twigs, 19 Monocotyledon samples, and 15 sediment samples.

The samples submitted to ORAU were prepared according to methods given in Hedges *et al* (1989) and measured as described in Bronk Ramsey *et al* (2004). Those submitted to Groningen were processed and measured as described by Aerts-Bijma *et al* (1997; 2001) and van der Plicht *et al* (2000). Both laboratories maintain continual programmes of quality assurance procedures, in addition to participation in international inter-comparisons (Scott 2003). These tests indicate no laboratory offsets and demonstrate the validity of the measurements quoted.

The results are presented as conventional radiocarbon ages (Stuiver and Polach 1977), and are quoted in accordance with the international standard known as the Trondheim convention (Stuiver and Kra 1986). The calibrations of these results, relating the radiocarbon measurements directly to calendar dates, have been calculated using the calibration curve of Reimer *et al* (2004) and the computer program OxCal (v3.10) (Bronk Ramsey 1995; 1998; 2001). The calibrated date ranges for these samples are given in Table 1 and have been calculated using the maximum intercept method (Stuiver and Reimer 1986). They are quoted in the form recommended by Mook (1986), with the end points rounded outwards to 10 years. The graphical distributions of the calibrated dates, given in outline in Figures 1–4, are derived from the probability method (Stuiver and Reimer 1993).

3.2.4.1 Sampling

The dating of environmental cores and monoliths can present various problems, most of which can be investigated through a rigorous programme of radiocarbon dating and sample selection.

3.2.4.2 Macrofossils

Although macrofossils are now often preferred as samples from environmental cores, as they can be identified as short-lived material, care must be taken when they come from aqueous environments (*e.g.* fluvial, alluvial, estuarine, etc). In these instances there is some possibility that the macrofossils were in-washed. While in-washing is more likely to bring in material that is of an older, rather than younger, date, wet-dry cycles and invasive reeds, such as *Phragmites,* present the possibility of younger material being brought down through the sediment column. Because of these potential problems, the radiocarbon programme employed is one with consistency as its foremost aim.

Consistency can be demonstrated in two ways. The first is through good overall agreement between the radiocarbon measurements and the core sequence. The second is through the replication of results from a specific level in the core. The replication of results is why it is preferred to have two macrofossils submitted from any given level, it is also part of the reasoning behind dating multiple fractions of peats, soils, and sediment, which are dealt with in the next section. If the resultant measurements are statistically consistent (*i.e.* $T'<3.8$, $\nu=1$) then it is probable that the two dates correctly date that level. When the two dates are not statistically consistent, the data need to be re-evaluated.

3.2.4.3 Sediment

The second type of material submitted for radiocarbon dating consisted of sediment. The dating of sediment and the reliability of the resultant dates from various fractions (e.g. humins, humic acids, etc) has been a topic of contention in the literature (see Blaauw *et al* 2004; Kilian *et al* 1995; 2000; and Shore *et al* 1995). The two most commonly dated fractions from these samples are the humins (i.e. alkali and acid insoluble organic detritus) and the humic acids (i.e. alkali soluble and acid insoluble matter). A third fraction that is sometime dated consists of the fulvic acids (i.e. the acid soluble fraction). Finally, if there is not enough available material to date the separate fractions then the bulk sediment can be dated (i.e. humin and humic fractions combined).

As the humin fraction is composed of the actual organic detritus, the resultant date from measuring this fraction is subject to many of the same processes that affect the dating of macrofossils in the same type of environment. Firstly, organic material that forms all or part of the humin fraction could be in-washed, which would result in a date that is too old. Contamination of this material by geological age carbon (e.g. coal, hard-water error) would have the same effect. The humin fraction can also be too young, if for example the environment is prone to wet-dry episodes or bioturbation, allowing intrusive material to work its way down the sediment column. Therefore, the humin fraction is not necessarily homogenous, and so it might be best to avoid dating this fraction by AMS as the smallest contamination would greatly affect the resultant measurement. Humins may better be dated through conventional radiocarbon dating techniques, as it is unlikely that a sufficient volume of such contamination would be present to bias such results significantly.

The second fraction that is often dated is the humic acids, which are the *in situ* products of plant decay. Although they are produced *in situ* and imply a stability to the ground surface, it has been shown that they can be mobile in groundwater, both vertically and horizontally (Shore *et al* 1995), but that their mobility is probably limited. Therefore, humic acids cannot be relied upon to always correctly date the level from which they were collected either. However, unlike the humin fraction, humic acids are homogenous, as they are alkali soluble, and therefore can be more reliably dated through AMS.

Fulvic acids are acid soluble and therefore can be suspended in a homogenous solution. Shore *et al* (1995) have shown that fulvic acids are nearly always the youngest fraction within a sediment profile. However, they also show that in a few cases they are by far the oldest of the three dated fractions at a level. They go on to suggest that this is likely due to the fact that fulvic acids are soluble in water and therefore are highly mobile, moving up and down with the water table and laterally within the subterranean drainage patterns.

In some cases, when there is not enough material for dating of separate fractions, the humic acid and humin fractions can be bulked together to provide an average date for all the organic material in that level. As stated earlier however, it is preferable to have the dates on the two fractions as this provides the data necessary for using replication as a measure of consistency. When the dates on two fractions are obtained, if they are statistically consistent, a weighted average can be taken before calibration as described in Ward and Wilson (1978). In most cases this creates a date that is more reliable. However, if the two results are not in agreement then the data need to be re-evaluated, in an attempt to determine which sample more reliably relates to the date of the level under consideration.

3.3 Dendrochronological dating

In total, 8 wood samples were collected for dendrochronological analysis from 6 large tree trunks recorded at Warren Farm Quarry, Lockington. The trees were interbedded within the sands and gravels, which on the basis of both geological geomorphological field mapping and analysis of LiDAR were assumed to be part of T1 (Hemington Terrace), aggraded during the mid Holocene. It is likely that all the tree trunks had been moved slightly during mineral extraction, though it appears from the available evidence that the majority were originally within 1-2m of the Mercia Mudstone rockhead. All the recorded trunks had intact root boles and none showed evidence for anthropogenic modification (e.g. tool marks), which suggests that they were incorporated into the channel through natural processes of riverbank erosion and tree throw on the floodplain. None of the sampled trunks were more than 50m apart. Samples were sent to the University of Nottingham for analysis.

3.4 Core stratigraphy, physical and chemical parameters

The palaeochannel cores and tins were subject to a rigorous scientific quantification of their physical and chemical parameters. The following parameters were measured:

3.4.1 Organic content

All cores and tins were sampled at 1cm contiguous samples along their entire length. Sediment from each sample was transferred to a labelled sample bag and freeze dried. After freeze drying samples were sieved in a 2mm stainless steel sieve. Crucibles were dried overnight at 109^{O}C to remove any excess moisture. The crucibles were weighed (a) and then approximately 1g of the $\leq$2mm soil fraction was added to each crucible. The crucibles were again dried overnight at 109^{O}C to remove any moisture from the sediment. The crucibles and samples were weighed (b) and then placed in a muffle furnace at 450^{O}C for 4 hours. The crucibles and soil sample were then weighed again (c). The % organic mater of the soil was then calculated using the formula:

$$\% \text{ Organic matter} = \frac{(a - c)}{(a - b) * 100}$$

3.4.2 Carbonate content

After the organic content had been burned off the samples, the crucibles were returned to the muffle furnace at 800^{O}C for a further hour. The crucibles were again weighed (d). The carbonate content of the sample was calculated through the formula:

$$\% \text{ carbonate content} = \frac{(c - d)}{(b - a) * 100}$$

3.4.3 Magnetic susceptibility

The magnetic susceptibility of the samples was measured through a Bartington MSII. A 10ml pot was then weighed (d), filled with the $\leq$2mm of sediment, then reweighed (e). The Bartington MSII was switched on for 30 minutes to warm up. Each sample was measured three times in the following sequence: Measurement of air (a), measurement of sample (b), measurement of air (c). The timing for each sample measurement was set at 30 seconds. The measurement of air samples allowed for the calibration of drift of the instrument.

From this data the average of the three readings was calculated for each sample via the calculation:

$$e - d = f$$

$$b1 - (a1 + c1) = g1$$
$$b2 - (a2 + c2) = g2$$
$$b3 - (a3 + c3) = g3$$

$$\frac{(g1 + g2 + g3)}{3} = h$$

$$\frac{h}{f} = \text{magnetic susceptibility units } (10^{-8} m^3 Kg^{-1})$$

3.4.4 Eh

The Eh of the samples was measured using an Alpha 500 contact probe. The instrument was switched on for 30 minutes to warm up. The contact probe was calibrated through immersion in a series of standard buffers at pH 4 and pH 7, whilst measuring the temperature of the buffer solution. Eh readings were made at 5cm intervals along the cores and tins through placing the probe into the sediment. The contact probe was washed thoroughly between readings. All Eh readings are given in millivolts.

3.4.5 pH

The pH of the samples was measured using an Alpha 500 contact probe. The instrument was switched on for 30 minutes to warm up. The contact probe was calibrated through immersion in a series of standard buffers at pH 4 and pH 7, whilst measuring the temperature of the buffer solution. pH readings were made at 5cm intervals along the cores and tins through placing the probe into the sediment. The contact probe was washed thoroughly between readings.

3.4.6 Geochemistry

Approximately 2g of the freeze dried $\leq$2mm fraction of sediment was accurately measured into a 100ml beaker. Three ml of concentrated Nitric Acid is added and the beakers warmed to dryness on a hotplate. The samples are removed and a further 3m of concentrated Nitric Acid and 0.5ml of concentrated Hydrochloric Acid is added. The samples are replaced onto a hotplate and removed on the appearance of brown nitrous oxide fumes.

The contents of the beakers were transferred to centrifuge tubes using distilled water and the tubes were centrifuged for 20 minutes at 2500 rpm. The supernatants were transferred into 25ml volumetric flasks, and the beakers were cleaned again with distilled water and the contents removed to the centrifuge tubes, which were then centrifuged at 2500 rpm for a further 20 minutes. The supernatants were added to the 25ml volumetric flasks and the pellets from the tubes discarded. The volumetric flasks were made up to 25ml using distilled water and the samples transferred to 30ml plastic labelled sample tubes. The concentration of the element cat-ions was made through Inductively Coupled Plasma Mass Spectrometry (Thermoelemental X Series). Each sample had its concentration measured 3 times and an average produced of the results. The average concentration for each element on each sample was converted to mg/Kg, though dividing the concentration by the sample mass.

3.4.7 Grain size

From the freeze dried $\leq$2mm fraction between 2 – 10g (depending on estimated sand content) was accurately weighed into a clean dry beaker. The soil is dried overnight at 90^{O}C. and then re-weighed to give the oven-dry weight. 10 ml of water is added to each sample with 5 ml of the hydrogen peroxide. 4. After 2 – 3 hours a further 5 ml of hydrogen peroxide is added and the sample allowed to stand overnight. The beakers were warmed on a hotplate (starting at 80^{O}C and gradually increasing the temperature to 100 ^{O}C) until the reaction is complete and there is a clear supernatant above the sample.

The beaker contents were carefully transferred to a weighed centrifuge tube, using a policeman rod to clean the sides of the beaker. The tubes are centrifuged at 2500 rpm for 1 hour. The centrifuge tube is dried overnight at 90^{O}C before being reweighed. Approximately 30 ml of the 0.4% sodium hexametaphosphate solution are added to each tube and initially disaggregated with a spatula. The soil suspension is screened through a 63µm sieve collecting the screened fraction in a 125 ml bottle. The centrifuge tube is washed with a small amount of the sodium hexametaphosphate and this is also passed through the sieve. The residue (>63 µm or >1000µm) and centrifuge tube were then washed with water, passing the washings through the sieve. The residue on that sieve was then washed until no more fines are washed through and all the sodium hexametaphosphate has been washed away. The residue is washed into a weighed dry 60 ml bottle with distilled water and dried overnight. This is then reweighed (and stored for sand fractionation if >63µm). The screened suspension was placed in an ultrasonic bath where it is treated for 5 minutes before being run on the MasterSizer (<63µm) or Digisizer (<1000µm).

3.4.8 Tin/core sediment stratigraphy

In addition to the quantification of the various chemical and physical parameters, selected cores/tins were subject to a qualitative assessment of their sediment stratigraphy. After cleaning each core had its stratigraphy recorded along its length. The recording of each sediment unit involved measuring its length, describing its composition in a subjective manner, e.g. a blue grey silty clay with a trace of sand, and also in a more objective way using the Troel Smith key, noting attributes such as elasticity, degree of stratification, etc. The colour of each sediment unit was recorded on a Munsel chart. This stratigraphic description was then drawn on scaled paper and scanned into Adobe Illustrator, so the core/tin stratigraphy could be viewed against graphs physical/chemical parameters.

3.4.9 Data ordering and analysis methods

All of the numeric data, e.g. organic content values, were entered into Excel spreadsheets, recorded by core/tin. Limited data analysis and graph production took place within the statistical analysis package SPSS.

3.5 Pollen and Spores Assessment

This sub-project was part of the palaeoenvironmental evaluation specified in the Phase II PD (Brown *et al.* 2004) which stated "Palaeoenvironmental analysis will include determination of routine sedimentary characteristics (organic and $CaCO_3$ content), analysis for pollen, spores and coleoptera which can provide details of the channel conditions, degree of canopy closure, the presence of grazing animals and other indicators of human presence." This aimed to provide a systematic evaluation of the differential preservation of pollen and spores in this typical area of exploitable floodplain aggregate.

Samples were taken from a spectrum of cores from palaeochannels chosen to represent the variation in age, position and environmental conditions within the study area. A list of the cores (Tab 3.1) and their locations are shown (Fig. 3.3).

Core Number	Total depth (m)	No. of samples	Estimated Age based on chrono-stratigraphic model	Determined age (base) Cal BC/AD Oldest used	Environment
MFC2		13	Post Medieval	800-510 BC	Low swale-like palaeochannel, below watertable, regularly flooded
T1C7	2.25	16	Late Prehistoric	840-780 BC	Large Soar palaeochannel in the middle of the regularly flooded area, under woodland, watertable maintained high as SSSI site
T1C12	2.14	13	Late Prehistoric	AD 890-1120	Large Soar palaeochannel in the middle of the regularly flooded area, under woodland, watertable maintained high as SSSI site
T1C10	1.88	13	Late Prehistoric	3030-2890 BC	Palaeochannel of the Soar at the edge of the modern floodplain and the regularly flooded, under grassland
TFGC14 (GCTF14)	3.8	9	Early-Mid Holocene	3640-3370 BC	Edge of the modern floodplain but associated with a channel crossing from low terrace into modern floodplain, under grassland
T1C14	0.9	6	Early-Mid Holocene	1390-1120 BC	Palaeochannel on low terrace
WFQC1 +	0.5	4	Early-Mid Holocene	1940-1740 BC	Warren Farm Quarry exposed palaeochannel on low terrace, at top of gravels
WFQCH1	0.74	2	Early-Mid Holocene	1940-1740 BC	Warren Farm Quarry exposed palaeochannel on low terrace, at top of gravels
WFQC2M1	0.5	4	Early-Mid Holocene	1060-890 BC	Warren Farm Quarry exposed palaeochannel on low terrace, at top of gravels
WFQC2M2	0.5	4	Early-Mid Holocene	1060-890 BC	Warren Farm Quarry exposed palaeochannel on low terrace, at top of gravels

WFQCH2M3	0.5	4	Early-Mid Holocene	1060-890 BC	Warren Farm Quarry exposed palaeochannel on low terrace, at top of gravels
WFQC3	0.5	4	Early-Mid Holocene	2860-2490 BC	Warren Farm Quarry exposed palaeochannel on low terrace, at top of gravels
WFQ5	0.5	4	Devensian	14980-14180 BC	Warren Farm Quarry exposed palaeochannel within terrace gravels, most southerly of all sample locations

Tab 3.1: Sites used for environmental sampling with number of pollen samples taken for assessment.

Of particular interest in this study was the concentration and preservation of the pollen and spores. There is a large literature on pollen and spore taphonomy and several different grain classification schemes. A discussion of this research can be found in Tinsley (2004) which is based upon a similar study of the pollen preservation in the Somerset levels as part of the Monuments at Risk in Somerset Project (MARISP) and a study of the effects of peat wastage in the Somerset Levels by Brown *et. al* (2003). Pollen preservation was recorded using a three fold classification adapted from Delcourt and Delcourt (1980); corroded, degraded and mechanically damaged. Where more then one form of degradation was present only the most developed was recorded. The results were condensed to pollen concentration, % unidentified and % degraded which included a summation of the Delcourt and Delcourt (1980) categories (section 6.2).

3.6 Coleopteran Assessment

The variability in sediment architecture and often complex depositional regime of alluvial deposits necessitates a sampling strategy that considers both the archaeological and environmental development of the site. With this in mind, a 'complete' sampling strategy was adopted at Warren's Farm Quarry, when recovering material for palaeoenvironmental analysis. Bulk samples (for insects) were recovered from sediments adjacent to samples collected for pollen analysis, recording the stratigraphy of the deposit locations, with the bulk sample areas being surveyed using differential GPS onto site datums. The aim was to provide a full, high resolution, environmental record at a site-specific level and elucidate *in-situ* environmental conditions during the period of alluviation and deposit formation.

Samples for palaeoentomological analysis were recovered from a series of seven palaeochannels in and around the quarry at Warren's Farm (Table 3.1). Sampling methods follow those recommended by Kenward (1978a, 1978b) and Kenward *et al*. (1980). Bulk samples of 10l were recovered from exposed palaeochannels WFQ1, 2, 3, 4, 5, and 6 within the quarry. The material was sampled at 10cm intervals from organic rich deposits overlain by sands and gravels or alluvium. Smaller samples, <500ml were also recovered from organic rich deposits using a manual auger from TFGC14 in approximately 20cm spits.

A further series of samples (Tab. 3.1), were extracted from palaeoecological cores in order to establish, if any, differential preservation of the insect remains between various palaeochannels across the study area. Bulk samples collected for Coleopteran evaluation were adjacent to the tin samples collected for pollen. Thus a depth of WQFC5 10cm, is the same for both pollen and Coleopteran evaluations.

3.6.1 Processing and Identification

The samples were processed using the standard method of paraffin flotation (Kenward *et al.* 1980, Coope and Osborne 1968). Preparation of samples for palaeoentomological analysis within the laboratory is a three-fold process. The final analysis of this material follows a series of guidelines developed, refined and disseminated over the past thirty years by Harry Kenward (e.g. 1974, 1975, 1976, 1978a, 1978b, 1982; Hall & Kenward 1990, Kenward & Hall 1995, 1997) and Mark Robinson (1981, 1983, 1993).

3.6.1.1 The Paraffin Flotation Technique

7kg/10l of each sample was placed in 15 litre plastic buckets and hot tap water was applied, where possible the material was left to soak overnight to facilitate disaggregation prior to sieving. A small amount of the sample was placed in a 300μm mesh sieve and hot tap water (40-50°c) was applied to remove the minerogenic matrix.

When washing was completed, the remaining organic detritus was allowed to drain in sieves for one hour. The sample was then returned to a clean bucket and the sample was covered with enough paraffin to produce a slurry when the paraffin was thoroughly incorporated. The material was allowed to stand for a few moments to allow the paraffin covered chitinous insect remains to float freely from the organic detritus, which are concentrated within the floating paraffin.

Fast flowing cold water was then added to the bucket, and the contents left to stand for one hour. The top twenty centimetres of the paraffin/water mixture were then poured through a clean 300μm mesh sieve. The process was repeated a total of three times at fifteen minute intervals, each time the bucket was refilled with cold water and the organic material stirred well. For the final pour, as much of the fluid was poured away as possible, before the residue in the base of the bucket is also poured into the sieve. The sample was then cleaned with domestic detergent to remove traces of paraffin from the flots. The sieve was then rinsed thoroughly until all traces of the detergent were removed. Finally, the flots were stored in airtight containers, with ethanol, to retard decomposition.

3.6.1.1 Sorting and Identification

The insect remains were then sorted from the paraffin flot and the sclerites identified under a low power binocular microscope at x10 magnification. Where possible, the insect remains were identified by comparison with specimens in the Gorham and Girling collections housed at the University of Birmingham. The taxonomy used for the Coleoptera (beetles) follows that of Lucht (1987).

3.6.2 The objective analysis, quantification and presentation of palaeoentomology as an environmental indicator

The remains of a wide variety of insects such as caddis flies (Order: Trichoptera), dragonflies (Order: Odonata), non-biting midges (Order: Diptera; Family: Chironimidae) and beetles (Order: Coleoptera) may be employed as palaeoenvironmental indicators. It is the robust remains of the beetle, however, which are currently the most commonly used, though research applying other families of insects is becoming increasingly common. Beetles are useful for several reasons:

- Their diversity.
- They are virtually ubiquitous.
- The robust character of their chitinous exoskeleton, which preserves exceptionally well.
- Distinguishing details that permit the identification of fossil material, in many cases to species level.
- Beetles, in the form in which we see them today, have been present for many millions years, as far back as the Carboniferous period.

In this instance, it is the application of beetles as ecological indicators that is of greatest importance. A great deal of 'habitat specific' and 'site specific' ecological inferences and data may be gained by examining the insect assemblages (Kenward, 1978). Species of beetle are dependent upon five criteria, which rely on species autecology and will subsequently effect species dispersal on a local scale (Elias, 1994):

- Botanical factors.
- Soil type.
- Microclimate.
- Hydrological conditions.
- Chemistry.

3.6.3 Difficulties with environmental interpretation using palaeoentomology

In many cases, the prime objective of any palaeoentomological analysis is to reconstruct the past events and ecological conditions which prevailed at a site during an episode of development and is ultimately based on the habitat requirements of the insects that are recovered (Kenward 1978).

Determining the past ecological conditions at a site is relatively easy. The species found within the sample are recorded, keys relating to the different taxa and reference books are then used to record the habitat in which this species is commonly found. This allows the establishment of the ecological conditions in the immediate vicinity of the deposit. From this it should be possible to quantify this habitat in the archaeological record e.g. one species from a particular environment = 1 area of this type of habitat being present nearby and thus the surrounding environment can be built up piece by piece. This is known as the 'mosaic' approach (Kenward 1978).

These simple concepts are however beset by a variety of problems that are highlighted by Kenward (1975). Further work by Kenward (1978) suggests six primary problems when interpreting archaeological material:

1. Establishing the ecological requirements and variety of habitats.
2. Gauging the number of species that have been transported some distance before any assumptions about the immediate environment are made.
3. Establishing the autochthonous fauna i.e. the component of the assemblage, which is derived from the area directly adjacent to the site.
4. Differentiating the living communities and the environments, which they inhabit, and the importance of these habitats to the overall reconstruction.
5. Establishing the importance of these habitats and their relationship to the site.
6. Establishing the age of the fauna and how/if this relates to the archaeology at the site.

Coupled with this is a series of further problems associated with species autecology and the overall ecology of the individual biome:

1. By their very nature some biomes will have a greater number of individual species associated with them than others (Kenward 1978).
2. Population densities of individual species will vary; added to this only limited information is available regarding modern population densities (Kenward 1978). This will lead to over and under-representation of both species and habitats within archaeological deposits.

It cannot be taken for granted that an assemblage is directly representative of a context over short spatial and temporal scales. It may represent weeks or even years of accumulation and represent a rapidly changing habitat (Kenward, 1978). Finally, the most significant problems lie with the basis of palaeoentomology itself, that of modern entomological study (Kenward 1978). In many cases modern work is limited and records of the modern ecological range of many species are inadequate or inaccurate. In some cases the habitats that these species dwell within are extremely broad (Kenward 1978) e.g. the entry for the Carabidae *Pterostichus strenuus* in Koch (1989a): "on loamy arable fields, meadows and weedy places; damp floodplains and woodland margins; moist turf; brick pits; wash zones on the coast. Under leaves, detritus, straw, moss and decaying vegetation; in flood debris and compost; under rotten bark; in mole nest". This taxa, which is commonly found in palaeoentomological assemblages, is extremely cosmopolitan.

3.6.4 A solution to problems of interpretation

To resolve this problem, Kenward has developed several paradigms that may be used to produce a more accurate interpretation of archaeological material. The method developed by Kenward (1978) which is most pertinent to this study, is the "Whole Assemblage" approach. The assemblage is examined in its entirety and the proportional significance of the components is used to draw conclusions about the environment (Kenward 1978). This method uses the general environments suggested by the majority of the insects recovered from within the individual sample as opposed to using the individual insect to draw such conclusions (Kenward 1978). If a single individual of a species has been recovered, whilst it may intimate some aspect of the habitat not suggested by other species, its overall value as an environmental indicator is limited.

This is not however, always the case and taking this approach on face value is slightly flawed and is related to the problem of over and under-representation in a single sample. Kenward (1978) suggests that greater importance should be attached to six large ground beetles that are generally found in low population densities, than a large population of Staphylinids that are commonly found in high numbers.

3.6.5 Visual Presentation of Data

Meaningful, visual presentation of this type of data is extremely difficult. To facilitate this, each species is designated an ecological code which corresponds to the primary habitat this species is associated with. The table used in this thesis is based on the work of Kenward (1978), Kenward and Hall (1995), Robinson (1981, 1983, 1993) and more particularly Smith, Osborne and Barrett (1997, 2000).

The calculations used to visually present the data are relatively simple, the total number of species assigned to a particular ecological group is expressed as a percentage of the whole fauna. Smith *et al*. (2000) varied this method slightly and expressed the aquatic fauna as a percentage of the entire fauna and the terrestrial fauna as a percentage of the non-aquatic species after Robinson (1981, 1983, 1993). The author felt that in this case where the relative hydrological conditions are particularly important also being examined, that true representation of the aquatic fauna in relation to the terrestrial fauna was of importance. The column marked "EG" on site species lists is "ecological groups" a series of broad groupings to which individual species have been assigned by Hall & Kenward (1990), Kenward & Hall (1995, 1997), Robinson (1981, 1983, 1993) and Smith *et al*. (2000) (Tab. 3.2).

Ecological Groups	
ws	waterside
a	aquatic species
rd	species primarily associated with drier organic matter
rt	species primarily associated with rotting organic matter
rf	species primarily associated with foul organic matter, often dung
g	species associated with grassland
l	species associated with woodland
m	moorland

Tab 3.2: Species ecological groups.

3.7 Field survey

As this project required a high level of fieldwork it is worth describing the main field methodologies, not already specifically covered elsewhere.

3.7.1 Section recording

The sections recorded in the quarry had sediment units recorded every 20cm along the sections, drawn from a line level. Datums were recorded on the level via differential GPS. The drawings were made at 1:50. The drawings were scanned into Adobe Illustrator for final presentation.

3.7.2 Field survey

All field survey was recorded in XY and Z dimensions using a differential GPS, with each individual field survey being assigned a new file and tied onto existing permanent points within the study area. All permanent points had a minimum of 6 hours static observation points collected for Rinex correction of actual position.

3.8 Electrical resistivity (ER) materials and methods

3.8.1 Geoprospection within alluvial environments

Geoprospection methods are finding increasing application within geoarchaeological investigations, due to their potential to identify sediment architectures that have high geoarchaeological potentials (Carey *et al.* 2006). In contrast to shallow geophysical prospection used in conventional archaeological practice, such as gradiometer and earth resistance survey, the application of geoprospection techniques in geoarchaeological surveys is not to identify anomalies that are thought to be distinctly cultural in origin, e.g. the plan of a Romano-British Villa. Instead the techniques are applied to understand the sediment and stratigraphic sequences of different geomorphological units, in order to identify the geomorphological units/sediment architectures that have the highest geoarchaeological potential, in both palaeoecological and cultural archaeological contexts.

3.8.2 GPR prospection within alluvial environments – a resume

Although the application of geoprospection within geoarchaeological survey is still in its infancy, GPR has been employed in geoarchaeological evaluations. As discussed in Brown *et al.* 2005, the application of GPR to find areas of high palaeo-ecological and geoarchaeological potential within alluvial environments is difficult, but coherent data capture is possible to aid in geoarchaeological assessments.

Ground penetrating radar surveys use pulses of Electromagnetic (EM) radio waves directed down into the soil profile from a transmitting antenna, in order to investigate subterranean features. When discontinuities are encountered some of these radio waves are reflected back towards the surface, whilst other waves travel further down into the soil profile until they meet other discontinuities. At the surface a receiving antenna measures the reflected waves. By measuring the time taken between emission of the radar pulse and reception back at the antenna it is possible to measure the depth of a discontinuity in the soil profile. Within a floodplain context the boundaries between different geomorphological units will be seen as discontinuities, due to their different physical properties, e.g. clay and gravel.

The process of estimating the depth of discontinuities within the soil profile is complicated by different dielectric constants found within different sediment units. The electrical properties of a sedimentary unit effect the time taken for the radar pulse to travel through that unit. The dielectric permattivity is a property of an electrical insulating material (dielectric) equal to the ratio of the capacitance of a capacitor filled with the given material to the capacitance of the identical capacitor filled with air. The specific capacitance of a vacuum is Eo = 8.85x 10^{-12} Farads per metre. The relative dielectric constant (Er) for air is 1 and is approximately 81 for fresh water (Radan User Manual Definition 2004, GSSI, 128).

Within an alluvial context the relative dielectric permittivity (RDP) of different sediment units is critical; which is the ability of a sediment to absorb, reflect and be permeated by, the radar pulse. If there is a significant change in RDP between two different geomorphological units, such as clay and gravel, then strong reflections will result at the interface of the two units. The GPR pulse will be dissipated by materials of high conductivity. Therefore, sediments with high clay and water contents cause rapid attenuation of the GPR signal and are often impenetrable to higher frequency antennas, such as a 200MHz antenna. Jol and Bristow (2003) revise GPR applications and practices for mapping sediments. One of their conclusions is that GPR is most effective in electrically resistive materials such as sand, gravel, peat and limestone but decreases in data quality are seen in highly conductive materials such as silt, clay and calcretes. Key factors that affect the RDP of an unconsolidated material can be listed as (mainly from Ekes and Friele 2003, 90):

- Pore size
- Sediment type
- Stratification
- Grain size
- Water content

It should be emphasised that although GPR survey can be used to identify and to some degree characterise sediment architecture, the mechanisms that affect the radar wave reflections are imprecisely understood. The reflection from an unconsolidated material will be a function of its water content below saturation levels; the water content itself being a function of the sediment properties (Van Dam *et al.* 2003, 257 – 273). If GPR survey is carried out over saturated sediments penetration will be limited.

In order to correctly calibrate the electric depth model created by the GPR it is important that the dielectric properties of the soil profile can be accurately estimated. This in practice is extremely difficult, as within alluvial environments any GPR transect is likely to cross a series of different geomorphological units, each having a different RDP. Therefore, a compromise has to be reached in the dielectric constant that is used. Within this project the dielectric constant of the soil was estimated through comparison with gouge core transects, which is a common method of calibration (for example see Bridge *at al.* 1998).

The gouge core transects allowed the depth of the alluvium overlying the terrace and modern floodplain gravels to be accurately measured across a whole GPR transect. The dielectric constant was then set, which identified the interface between the alluvium and the gravels at the same depth recorded by the gouge core transect. This represents a compromise on setting the dielectric constant as the calibration is taking place within an alluvium unit, not combining the average of the alluvium and gravel units. However, the gravels are

impenetrable without powered coring equipment and thus the described compromise was reached through using gouge core data.

The identification of radar terminations is the basis for constructing a relative chronology for a sequence of sediment units (Bristow *et al*. 2005, 316*)*. Interfaces between different geomorphological units, e.g. a silty clay unit overlying a gravel unit, represent terminal events in either deposition or erosion processes and the start of subsequent processes. Although the ages of these sediment units cannot be ascertained without absolute dating methods, relative sequences can be constructed through studying the form of the interfaces seen. This has specific importance in geoarchaeological studies of alluvial environments where erosion and deposition by channels will have both destroyed and preserved the archaeological resource.

The heterogeneity of alluvial deposits allows discontinuities to be mapped and stratigraphies to be created. This property causes special considerations for GPR survey of alluvial environments. River floodplains are heterogeneous in both X, Y and Z dimensions. Upper terraces may have gravels close to the surface, with a thin covering of alluvium, whilst modern floodplains may have a considerable degree of alluvial deposition on gravels or bedrock. Palaeochannels may have high water contents, high clay contents, with organic rich pockets. Gravel architecture can vary radically between clast to matrix supported.

For GPR survey this can be problematic, in respect of data collection and real time amplification of signal. Consider two very different units that are surveyed within the same area, such as a gravel terrace and a palaeochannel with a fill of high clay content. The gravels in the terrace will have low absorption but high reflectance properties. Conversely, the palaeochannel will have low reflectance but high absorption properties, causing rapid attenuation of signal. In such cases, which are frequently encountered in alluvial environments, the different geomorphological units require a different amplification of signal. The amplification of the radar pulse is controlled through a gain applied to the signal. The level the GPR gain (amplification) is set at will be a compromise between obtaining good penetration in a series of different sediments and collecting clipped data, where the amplification of the signal has been too great and the minimum and maximum values are not realised. When considering alluvial stratigraphy it is often the contrast between different sediment units that is most important. Therefore, relative change and difference is as important for data collection within heterogeneous environments as absolute values.

From the phase I study of Predictive Modelling of Multi-period Geoarchaeological Resources at a River Confluence, GPR was shown to be effective at mapping the depth of alluvium above the gravels, the composition of the upper gravel deposits and identifying boundaries and variation between gravels and palaeochannels on the modern floodplain, terrace 1 and terrace 2. Conversely, the GPR penetration into the palaeochannels was generally poor. When palaeochannels had high water/clay contents, GPR was ineffective at mapping sediment structure. Therefore, GPR cannot be used to investigate the stratigraphy of high water/clay content palaeochannel fills, which are likely to be the palaeochannels that have the highest palaeoenvironmental potential. However, by using this criteria, palaeochannels that cause rapid attenuation of the radar signal should be earmarked for palaeoenvironmental sampling, due to the nature of the fill causing the loss of signal.

The two and three dimensional GPR surveys recognised distinct sedimentary structures in the heterogeneous alluvium deposits. Sedimentary units were interpreted according to their

reflection pattern and interpreted shape. The reflection amplitudes that were recorded related to differences in the sedimentary architecture of different geomorphological units. However, it was not possible to unambiguously predict the physical properties of a geomorphological unit from GPR reflection data. In general it was possible to differentiate between alluvium, palaeochannels, gravel and variations within the gravel, through changes in their relative RDP and hence reflectance pattern. However, in some cases different sedimentary units gave similar patterns of reflectance, e.g. gravels were generally seen as units of high reflectance but some clay layers produced a very similar reflectance pattern.

3.8.3 ER prospection within alluvial environments

After assessing the results from the GPR surveys during phase I of the project, it was decided to use other deep geoprospection techniques to compliment the GPR data. Electrical resistivity (ER) was selected to investigate palaeochannel stratigraphy and act as a comparative technique to GPR. Whilst GPR survey has shown to be incapable of penetrating clay filled palaeochannels there were sound reasons for expecting that ER could be successfully used to investigate palaeochannel sediments. This said, there are fundamental differences between ER survey and GPR survey and these have to be considered when the two techniques are compared.

3.8.4 An introduction to ER survey

ER survey uses electrical currents injected into the soil profile from a transect of electrodes to investigate subterranean features, via the resistance of different materials to the injected current (measured as ohms.m). When discontinuities are encountered (such as adjacent sediment units) there is expected to be a difference in resistivity values, due to differences in sediment architectures affecting factors such as grain size, water content, ion content, etc, which all contribute to the ability of a sediment to conduct electrical currents. The purpose of ER surveys is to determine the subsurface resistivity distribution. Electrical resistivity surveys have been used for many decades in hydrogeological, mining and geotechnical investigations. More recently, they have been used for environmental surveys and has also found recent application in geoarchaeological surveys (Bates 2007).

The following description of electrical resistivity imaging is derived from Loke (1999) unless otherwise referenced, which provides a comprehensive overview of ER, different electrode arrays and software options. Resistivity measurements are achieved by injecting current into the ground through two current electrodes (C1 and C2), and measuring the voltage difference at two potential electrodes (P1 and P2) (Fig. 3.9).

From the current (I) and voltage (V) values, an apparent resistivity (*pa*) value is calculated.

$p_a = k\ V / I$

where k is the geometric factor which depends on the arrangement of the four electrodes.

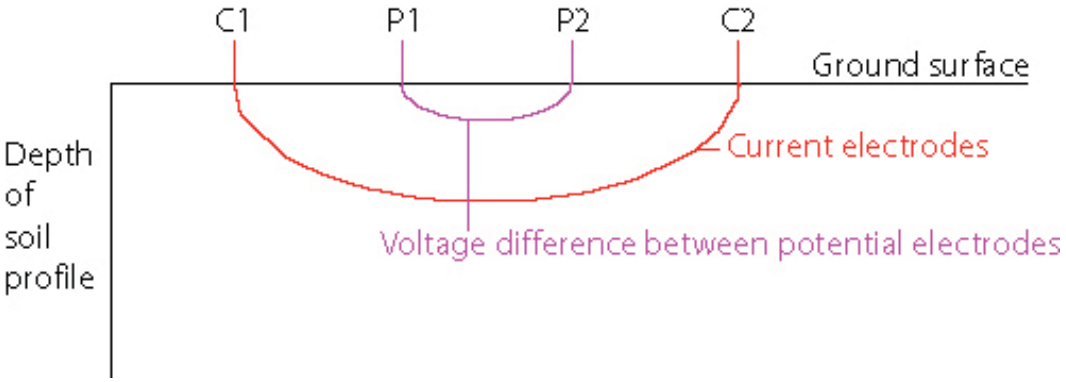

Fig 3.9: The basis of a resistivity measurement. Current is injected into the ground through C1and C2 and the voltage difference at two potential electrodes is measured at P1 and P2.

Resistivity meters normally give a resistance value, R = V/I,

The apparent resistivity value is calculated by
$p_a = k\ R$

The calculated resistivity value is not the true resistivity of the subsurface, but an "apparent" value that is the resistivity of a homogeneous ground that will give the same resistance value for the same electrode arrangement. The relationship between the "apparent" resistivity and the "true" resistivity is a complex relationship. To determine the true subsurface resistivity, an inversion of the measured apparent resistivity values needs to be undertaken.

3.8.3.1 Electrical resisitivity and sediment stratigraphy

Resistivity surveys provide information on below ground sediment architectures through estimating their resistivity distributions. Whilst it is clearly not possible to assign a particular resistivity value to a particular sediment type, i.e. 53.1 ohms.m equates to an organic rich clay, understanding the resitivity values of different sediments aids in interpreting ER sections.

With GPR the RDP of a sediment unit is important in understanding how the radar pulse acts within the soil and also how to interpret the resulting GPR section. Likewise the RDP of a sediment unit will determine its ability to conduct an electrical voltage, which can be measured in ohms.m. Therefore, the RDP of a sediment unit is also crucial in interpreting ER sections and identifying different sediment units.

In a general context, igneous and metamorphic rocks typically have high resistivity values. Sedimentary rocks, which usually are more porous and have a higher water content than igneous and metamorphic rock formations, normally have intermediate resistivity values. Wet soils and fresh ground water have lower resistivity values. This is a very general rule though, as, the resistivity of rocks and soils can vary by several orders of magnitude over relatively small areas. Broad resistivity values for a variety of geological samples and some soils are

given (Tab. 3.3), which are coded as high resistance materials (red), intermediate resistance materials (green) and low resistance materials (blue).

This general classification is of limited use when considering the study area of the Trent/Soar, especially as some of the terminology is ambiguous, i.e. what is the difference between clay and alluvium? The general stratigraphy of the study area is known in both geological and pedological contexts. Therefore, it is possible rank the different sediment units as encountered within the study area on a *pre-hoc* basis, dependent on their predicted resistivity values (Tab. 3.4).

Igneous and metamorphic rocks	**Resistivity range (ohm.m)**	**Conductivity (Siemen/m)**
Granite	$5 \times 10^{3} – 10^{6}$	$10^{-6} – 2 \times 10^{-4}$
Basalt	103 - 106	$10^{-6} – 10^{-3}$
Slate	$6 \times 10^{2} – 4 \times 10^{7}$	$2.5 \times 10^{-8} – 1.7 \times 10^{-3}$
Quartzite	$10^{2} – 2 \times 10^{8}$	$5 \times 10^{-9} – 10^{-2}$
Sedimentary rocks	**Resistivity range (ohm.m)**	**Conductivity (Siemen/m)**
Sandstone	$8 – 4 \times 10^{3}$	$2.5 \times 10^{-4} – 0.125$
Sandstone	$8 – 4 \times 10^{3}$	$2.5 \times 10^{-4} – 0.125$
Shale	$20 – 2 \times 10^{3}$	$5 \times 10^{-4} – 0.05$
Limestone	$50 – 4 \times 10^{2}$	$2.5 \times 10^{-3} – 0.02$
Soils and waters	**Resistivity range (ohm.m)**	**Conductivity (Siemen/m)**
Clay	1 – 100	0.01 – 1
Alluvium	10 – 800	$1.25 \times 10^{-3} – 0.1$
Groundwater (fresh)	10 – 100	0.01 – 0.1

Tab: 3.3: General resistivity and conductivity values of some rocks and soils (modified from Keller and Frischknecht, Daniels and Alberty 1966).

General sediment unit	**Resistivity ranking**
Clast supported gravel	↑ Highest resistivity values
Matrix supported gravel	
Sand	
Mercian mudstone	
Clayey sand	
Clayey silt	
Sandy clay	
Silty clay	Lowest resistivity values
Clay	

Tab 3.4: Table of predicted resistivity ranking of sediment units within the study area, on a *pre-hoc* basis before survey.

This table is constructed from the principles discussed above, where sediment units with a smaller clast size and higher water contents have a lower resitivity through being more

conductive. Therefore, a waterlogged clay will have a lower resistivity value than clast supported gravel.

Within a geoarchaeological context, the actual resistivity of the sediment unit in question then starts to take on a predictive capacity. Factors that influence the preservation of organic remains in alluvial environments, both in palaeoecological and cultural contexts, produce sediments with low resistivity values. Such factors are primarily water logging and small clast/grain sizes causing low redox conditions. Conversely, areas of high resistance can indicate other sediment units, which have different geoarchaeological potentials. High resistance features can indicate sands and gravels, which in alluvial Holocene records can have high geoarchaeological potentials. For example a wealth of archaeological remains were found at Hemington within gravels features including fish dams, fish baskets and medieval bridges (Cooper 2003: Salisbury 1992). Therefore, the interpretation of different resitivity values and their relationships to different sediment units potentially has a large role to play in geoarchaeological investigations.

3.8.4 ER materials and methods

3.8.4.1 Instrumentation and data collection parameters

The IRIS Syscal junior system was the switching unit employed to automatically select the four electrodes for any single measurement. This system has a maximum capacity of 48 electrodes in any single transect, collecting measurements via two cables which can both be attached to up to 24 electrodes. The IRIS Syscal Junior was programmed through Electre II. The Wenner Schlumberger array was selected. The data collection parameters were a stack of min 3/max 6, with a measurement time of 1000ms.

Whilst there are sound theoretical reasons to expect ER to provide good data on subsurface stratigraphy, the survey parameters determine the success of any geophysical survey. When using ER there are two principle factors to consider in the instrumentation set up, being the electrode array and the electrode spacing.

The Wenner Schlumberger array was selected after considering depth of investigation and data resolution. This is a hybrid between the classical Wenner array and the Schlumberger array. This array is moderately sensitive to both vertical and horizontal structures, representing a good compromise between the Wenner and Schlumberger arrays. The Schlumberger array is commonly used in resistivity sounding surveys. A modified form of this array, so that it can be used on a system with the electrodes arranged with a constant spacing is shown in (Fig. 3.10). Note that the "**n**" factor for this array is the ratio of the distance between the C1-P1 (or P2-C2) electrodes to the spacing between the P1-P2 potential pair. The sensitivity pattern for the Schlumberger array (Fig. 3.5.2) is slightly different to the Wenner array, with a vertical curvature below the centre of the array and slightly lower sensitivity values in the regions between the C1 and P1 (and also C2 and P2) electrodes. There is a slightly greater concentration of high sensitivity values below the P1-P2 electrodes. This means that this array is moderately sensitive to both horizontal and vertical structures.

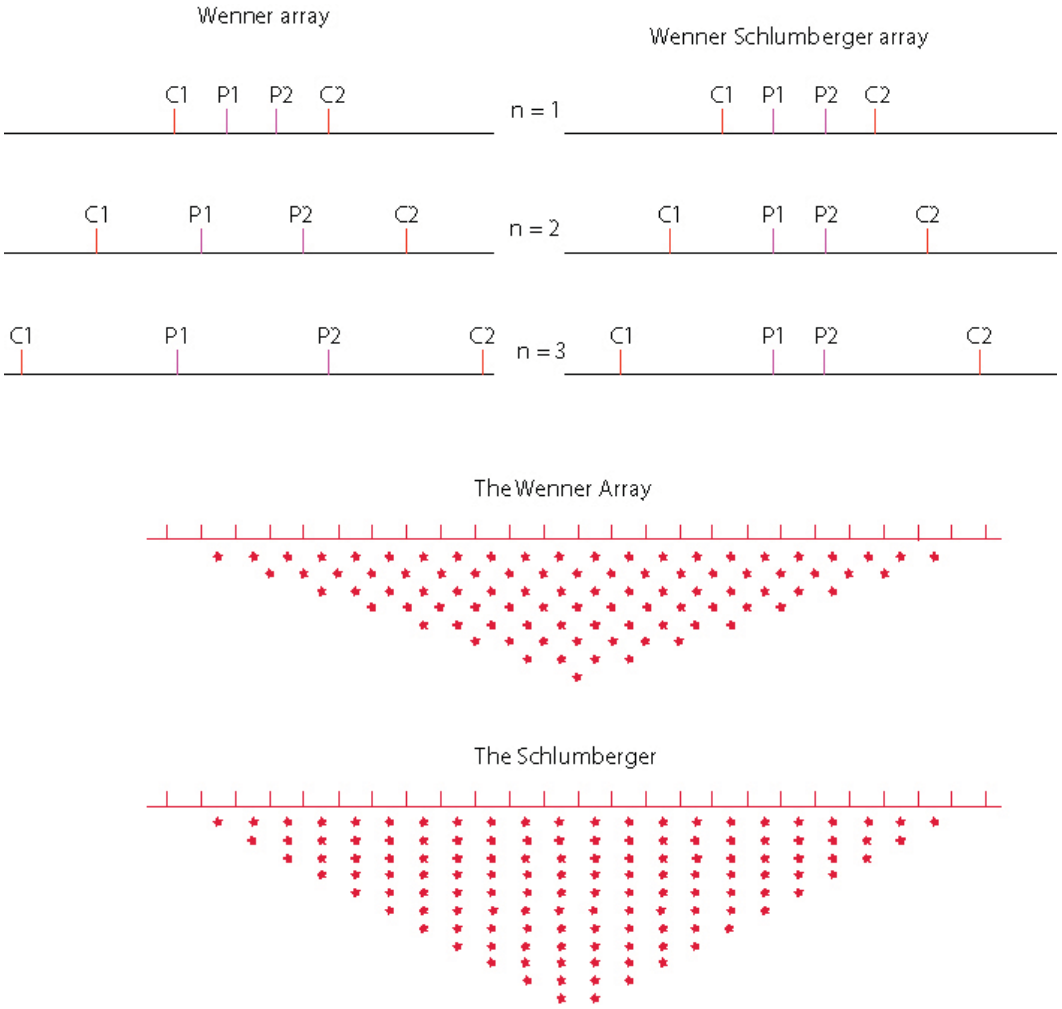

Fig 3.10: The Wenner and Schlumberger arrays.

The apparent resistivity value for the Wenner-Schlumberger array is given by

$$r = pi\ n\ (n+1)\ a\ R$$

where R is the measured resistance, a is the spacing between the P1 and P2 electrodes and n is the ratio of the distances between the C1-P1 and the P1-P2 electrodes. This array effectively becomes the Schlumberger array when the n factor is greater than 2. Thus it is actually a combination of the Wenner and Schlumberger arrays adapted for use for an arrangement with a line of electrodes with a constant spacing (as normally used in 2-D electrical imaging). Besides better horizontal coverage, the maximum depth of penetration of this array is about 15% larger than the Wenner array. Note that the normal Wenner array is actually a special case of the Wenner-Schlumberger array where the n factor is equals to 1.

The electrode spacing represents the compromise between the depth of penetration and data resolution by depth. From the borehole modelling, gouge core transects and section recording, the general stratigraphy of the study area was known. Therefore, the three electrode spacings of 0.5m, 1m and 2m were selected, keeping the number of data

measurement points equal in each. These three electrode spacings were compared in different situation across the study area to assess the effectiveness of ER in revealing alluvial sediment stratigraphy.

Using the 0.5m electrode interval 12 depth levels were used, giving 342 quadripoles (measurement points) for the first transect (Fig. 3.11). This gave a total first transect length of 23.5m. In order to avoid saw toothing and maintain depth and data resolution subsequent transects were 5.5m long, with the same 12 depth levels, that joined to the first transect of 23.5m (Fig. 3.12).

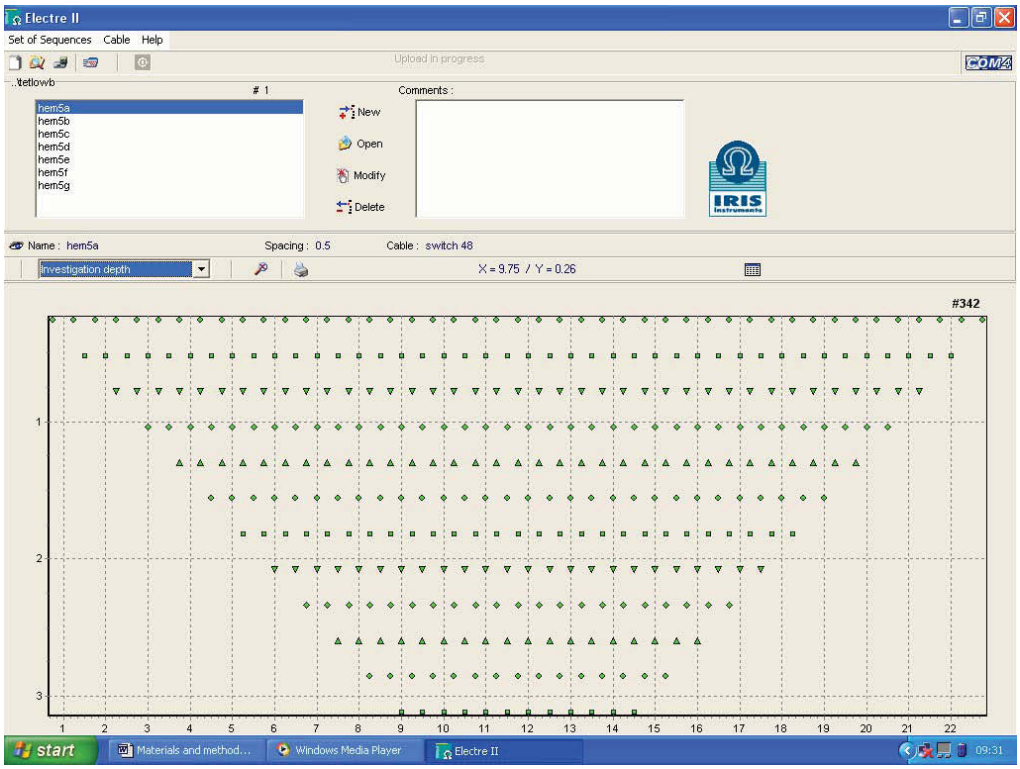

Fig 3.11: The data collection points on the 0.5m electrode spacing first transect.

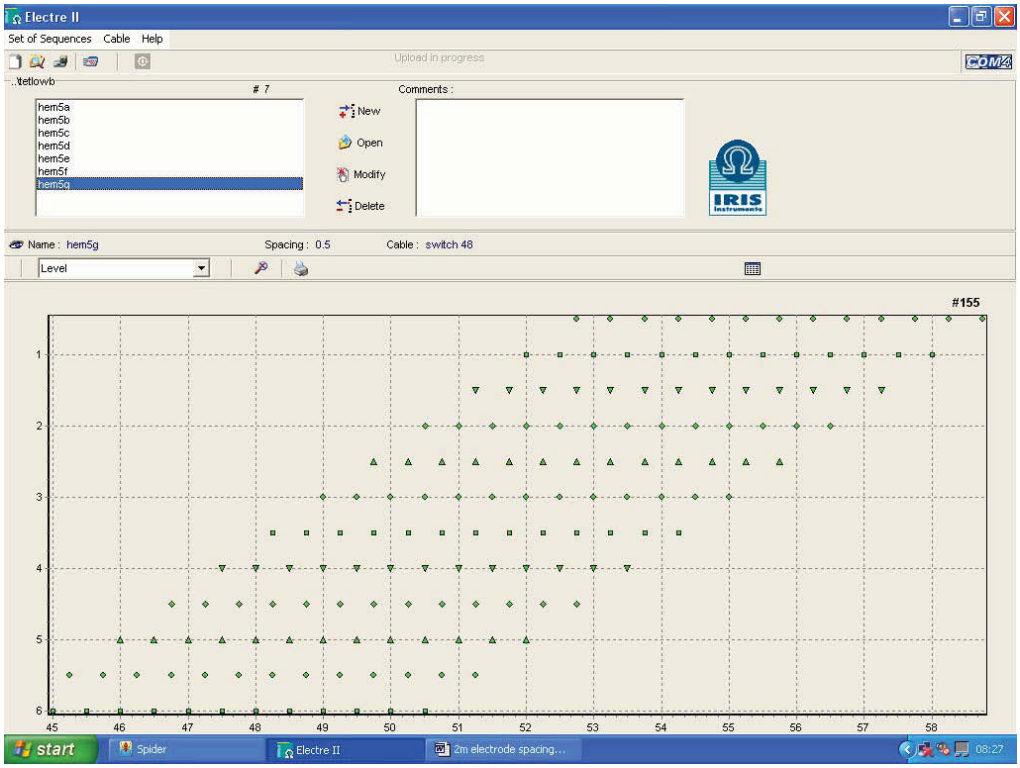

Fig 3.12: The data collection points on the 0.5m second and subsequent transects.

Using the 1m electrode interval 12 depth levels were used, giving 342 quadripoles (measurement points) for the first transect (Fig. 3.13). This gave a total first transect length of 47m. In order to avoid saw toothing and maintain depth and data resolution subsequent transects were 11m long, with the same 12 depth levels (Fig. 3.14). The same parameters were used for the 1m electrode spacing.

Using the 2m electrode interval 12 depth levels were used, giving 342 quadipoles (measurement points) for the first transect (Fig. 3.15). This gave a total first transect length of 95m. Only one 2m electrode interval transect was used in the study.

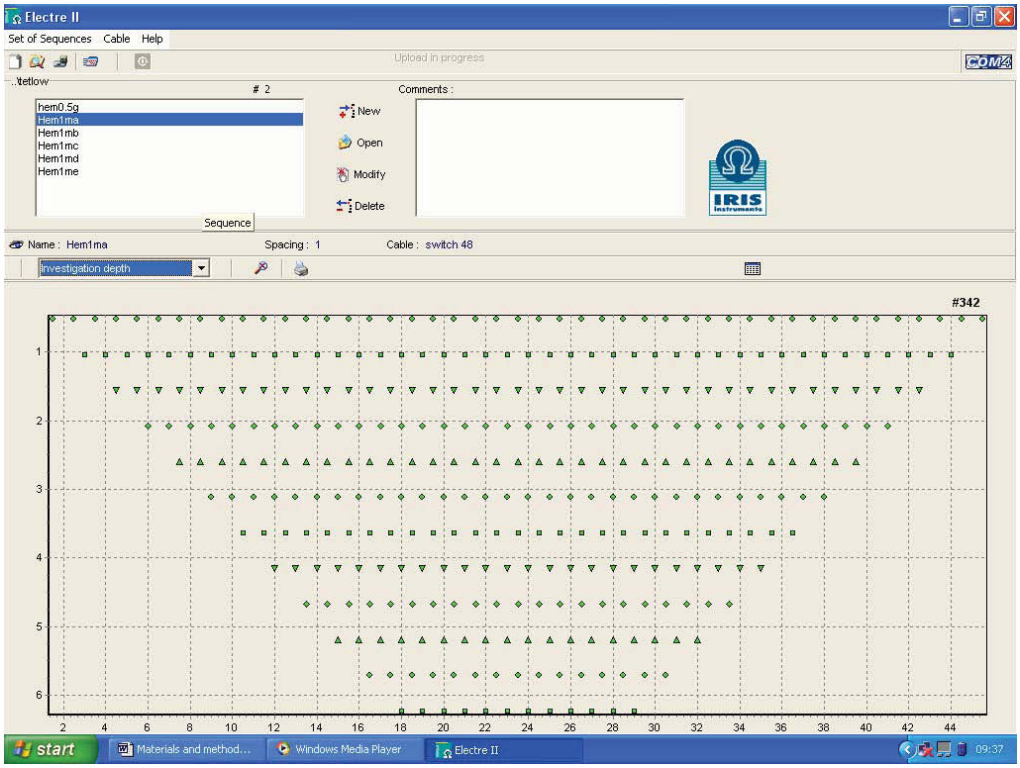

Fig 3.13: The data collection points on the 1m electrode spacing first transect.

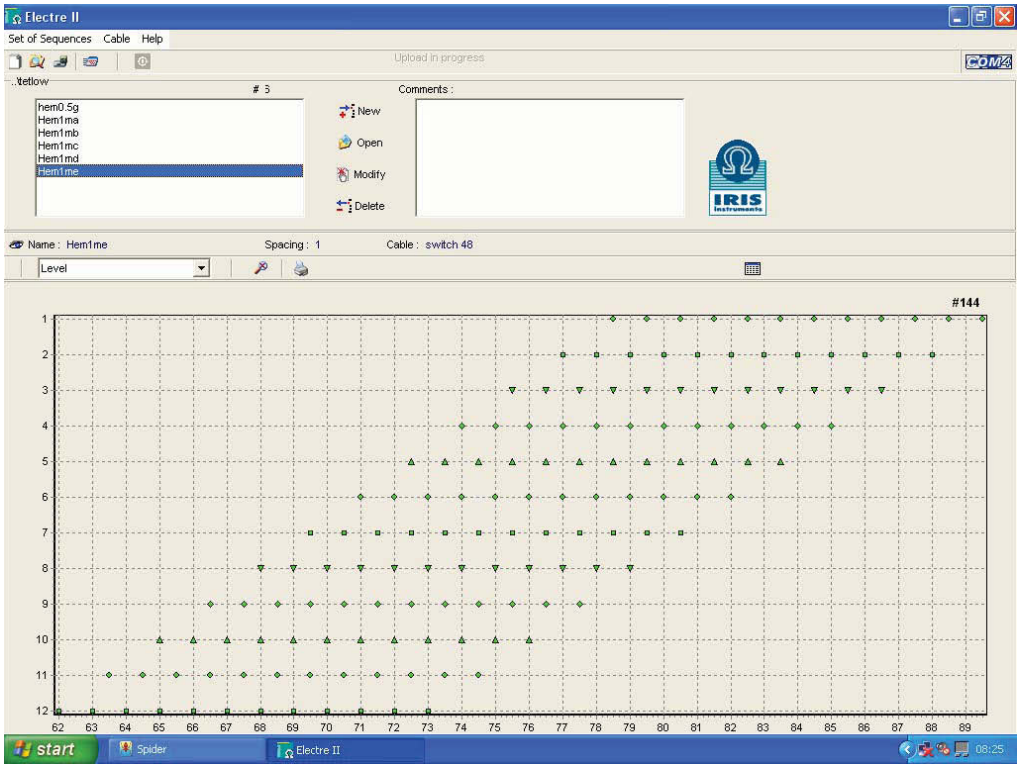

Fig 3.4: The data collection points on the 1m electrode spacing second and subsequent transects.

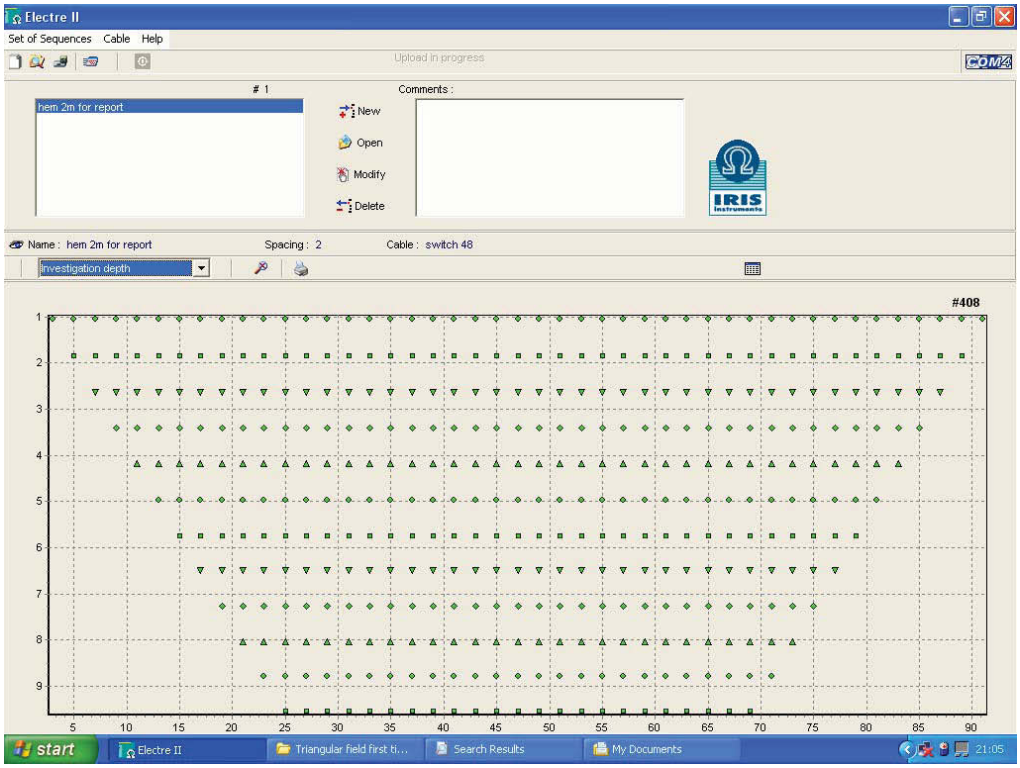

Fig 3.15: The data collection points on the 1m electrode spacing first transect.

3.8.4.2 Field methodology

The IRIS Syscal Junior was programmed directly from the PC with the files created in Electre II. Set up for the ER transects involved setting out a transect using ranging rods over selected features. Tapes were laid along the transect and then electrodes were placed at either 2m, 1m or 0.5m intervals. Two cables are employed with the Syscal Junior unit, each having 24 connections to attach to the electrodes via a wire with crocodile clips (Fig. 3.16).

On some ER sections GPR profiles were created along the same transects. Most transects had a gouge core taken at 10m intervals along the transect. The location of all ER, GPR and gouge cores were recorded using differential GPS and tied onto existing base stations within the study area. The ER sections were had their location recorded using differential GPS (Fig. 3.17).

Fig 3.16: ER transect running across a palaeochannel on the lower floodplain. The IRIS Junior unit is central between the two cables. Each cable is attached to 24 electrodes.

Fig 3.17: Recording the position of the ER transect T1F using dGPS.

3.8.4.3 Data download and pseudosection viewing

All data from the Syscal Junior was downloaded into the program Prosys II. Here the data was viewed as a pseudosection to assess data integrity and exported in a file format that could be viewed in RES2DINV. To visualise the data from a 2-D imaging survey, the pseudo-section contouring method is used. The horizontal location of a point is placed at the mid-point of the set of electrodes used to make that measurement. The vertical location of the plotting point is placed at a distance that is proportional to the separation between the electrodes. The pseudosection gives an approximate picture of the true subsurface resistivity distribution. However, this picture is distorted as the shape of the contours depends on the type of array used, in addition to the true subsurface resistivity.

In order to understand the true resistivity of the subsurface there has to be inversion of the ER data. At its simplest level inversion methods try to find a model for the subsurface whose response agrees with the measured data. The inversion subroutine tries to reduce the square of the difference between the measured and calculated apparent resistivity values. Besides trying to minimise the difference between the measured and calculated apparent resistivity values, the inversion method also attempts to reduce other quantities that will produce certain desired characteristics in the resulting model. Additional constraints help to stabilise the inversion process.

3.8.4.4 Data inversion

All data inversion was undertaken in the dedicated RES2DINV program. The data was initially viewed as a line plot to visually search for erroneous data points, with these being removed from the data set. The modified file was resaved. The data inversion used the Robust constraint (section 3.8.3.4). Inversion of ER data is a subjective process, due to non-uniqueness of data. If two different constraints are applied to the same data set, two different results can be produced. For the same data set, there is a wide range of models giving rise to the same calculated apparent resistivity values. To narrow down the range of possible models, some assumptions are made concerning the nature of the subsurface that are incorporated into the inversion.

When considering the application of inversion methods to data sets collected in alluvial environments, the nature of the boundaries between sediment units is critical, as the selected constraint method will model boundaries between units in different ways. For example are gradational or sharp boundaries or both expected within an ER data set? Furthermore, are these boundaries primarily expected in horizontal, vertical or both dimensions? All of these factors will influence the decision on the inversion method used.

To undertake the data inversion a least squares inversion was used, with a ‘robust constraint’. The least-squares inversion method attempts to minimise the square of difference between the measured and calculated apparent resistivity values. This method normally gives reasonable results if the data contains random or "Gaussian" noise. However if the data set contains outlier data points (where the noise comes from non-random sources such mistakes or equipment problems), this criteria is less satisfactory. Such outlier data points could have a great influence on the resulting inversion model. To reduce the effect of such outlier data points, an inversion method where the absolute difference (or the first power) between the measured and calculated apparent resistivity values is minimised can be used (Claerbout and

Muir 1973). There is a pcut-off factor which controls the degree in which this robust data constrain is used. If a value of 0.05 is used, this means the effect of data points where the differences in the measured and calculated apparent resistivity values are much greater than 5 percent will be greatly reduced.

The conventional smoothness-constrained least squares method (deGroot-Hedlin and Constable 1990) attempts to minimise the square of the changes in the model resistivity values. This will produce a model with a smooth variation in the resistivity values. This will produce a smoothed contour change, even when adjacent contours (or data points) have radically different values, such as the change between a fine clay unit and a coarse sand unit.

The robust model constrain inversion method, used on the model resistivity values, attempts to minimise the absolute changes in the resistivity values. This constraint tends to produce models with sharp interfaces between different regions with different resistivity values, but within each region the resistivity value is almost constant. This type of inversion method has clear application within alluvial environments.

Within alluvial environments there can be large differences between the measured and calculated resistivity values caused by non random sources, creating a data set with significant outliers. Such data sets that could contain a large degree of variance are where there are adjoining geomorphological units with radically different sediment architectures, such as were a silt clay palaeochannel joins terrace gravels with a shallow silty clay alluvial covering. In such examples a sharp boundary exists in resistivity relating to sediment architecture and should be modelled as discrete units.

In addition it was decided that the relative weights of the horizontal and vertical filters should not be changed. The relative weight of these filters can be changed when stratigraphy is expected to vary in only one dimension, such as temporal (depth) geological stratigraphy. In such a situation the vertical flatness filter is given a greater weight than the horizontal filter, allowing greater clarity in the stratigraphy of the section. However, geomorphological stratigraphy can vary in both X,Y (horizontal/spatial) and Z (temporal/depth) dimensions. Therefore, the relative weights of the horizontal and vertical filters were kept equal during the inversion. Finally the data was exported from RES2DINV as a bitmap and placed into Adobe Illustrator for final presentation.

3.8.4.5 Data interpretation

All ER sections had an interpretation made. Interpretation is a subjective process and in as much the identification of the geomorphological features was kept as simple as possible. Line drawing interpretations were placed on top of the ER sections, after gouge core stratigraphy and GPR sections ad been compared to the ER section.

3.8.6 The aims of ER survey within this study

The aims of the electrical resistivity survey can be summarised as:

- To investigate the capacity of ER to identify sediment stratigraphies on areas of terrace.

- To investigate the capacity of ER to identify sediment stratigraphies within palaeochannels.

In order to achieve these aims the following types of survey were applied.

1. ER transect compared to gouge core stratigraphy.
2. ER transect compared to GPR survey.
3. ER survey compared to both GPR and gouge core survey.
4. Assessment of ER on terrace 2.
5. Assessment of ER on terrace 1.
6. Assessment of ER on the modern floodplain.
7. Assessment of different depth penetrations of ER.

In order to achieve these aims a series of different ER transects were undertaken (Tab 3.5).

ER transect	Geomorphology	Electrode spacing	Other data on transect
T2A	Area of terrace 2, no palaeochannels visible through surface topography	1m	
T1A	Area of terrace 1, no palaeochannels visible through surface topography	1m	GPR, gouge cores, LiDAR
T1B	Area of terrace 1, no palaeochannels through surface topography	0.5m	GPR, gouge cores, LiDAR
T1C	Palaeochannel on terrace 1	1m	GPR, gouge cores, LiDAR
T1D	Palaeochannel on terrace 1	0.5m	GPR, gouge cores, LiDAR
T1E	Area of terrace 1 with palaeochannel	1m	Gouge core, earth resistance survey, LiDAR, ground based NIR scanning
T1F	Area of terrace 1 with palaeochannel	1m	
T1G	Palaeochannel marking the boundary between terrace 1 and terrace 2	0.5m	Gouge cores
T1H	Area of terrace 1 with palaeochannel	0.5m	GPR, gouge cores
T1J	Area of terrace 1 with palaeochannel	1m	GPR, gouge core
T1K	Area of terrace 1, no palaeochannels visible through surface topography	2m	GPR, gouge core
MFA	Area of modern floodplain with palaeochannels	1m	
MFB	Area of modern floodplain with palaeochannels	0.5m	

Tab 3.5: ER surveys undertaken.

3.9 Standardised keys for stratigraphy descriptions

The following key has been used throughout for sediment descriptions (Fig. 3.18).

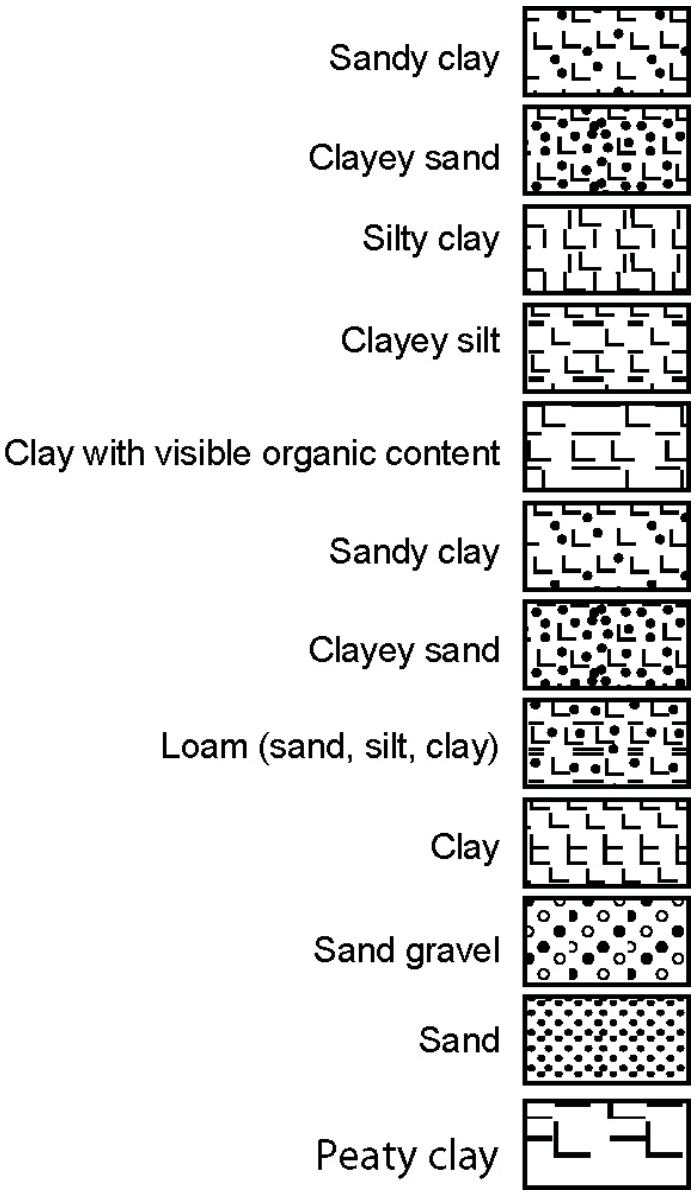

Fig 3.18: Modified Troel Smith key for sediment descriptions.

3.10 LiDAR intensity ground scanning

3.10.1 Introduction

This part of the project aimed to investigate the backscattered laser intensity data produced as a by-product of the airborne LiDAR elevation survey of the site, to determine whether soil and sediment properties might influence the reflection of the laser pulse. This chapter summarises the results of research at Lockington during 2006.

Airborne LiDAR provides access to high resolution, high accuracy terrain information and as a secondary output a laser "image" of the land surface derived from measurements of the intensity of reflection of each backscattered laser pulse. Archaeological applications of LiDAR have focused largely on its ability to provide a high resolution record of terrain variation, allowing the detection and mapping of subtle archaeological features, mapping of fluvial geomorphology and its unique ability to penetrate vegetation cover to map underlying archaeological earthworks.

Backscattered laser intensity measurements have largely escaped attention, and indeed do not form a part of the standard data product supplied by Environment Agency (EA; although intensity data is collected on each EA flight and can be accessed by reprocessing original flight data). The LiDAR system used by EA, NERC and many UK-based commercial LiDAR providers, including that used for the present project, an Optech Airborne Laser Terrain Mapper, operates in the near infra-red (NIR: 1047nm) and so backscattered intensity is in-effect a record of the reflectance of earth surface materials at this wavelength.

Initial examination of backscattered laser intensity in stage one of the project suggested that a fall-off in the intensity of the reflected light corresponds with the position of sediment filled landform features such as palaeochannels (Figs. 3.19 3.20 and 3.21). Variations in the reflectivity of various earth surface materials to laser light of differing wavelength are well-documented and damp soil conditions are known to reduce reflectivity. It was therefore postulated that the increased soil-moisture associated with palaeochannels, and perhaps other associated variations in soil and vegetation properties, are responsible for the reduced reflection of the laser pulse.

Limited work in stage one of the project examined laser intensity in relation to volumetric soil moisture measured *in-situ* at topsoil and subsoil level with a theta probe. The present work extends this research to consider the relationship between intensity and topsoil moisture more extensively across the site and to investigate the relationship between intensity, topsoil moisture and topsoil organic content in representative geomorphological units across the study area.

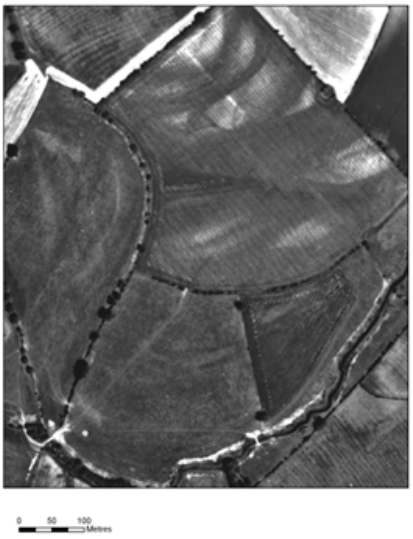

Air-photo

LiDAR Elevation (LPG)

LiDAR Intensity (LPI)

Fig 3.19: Air-photographic, LiDAR elevation and LiDAR intensity data for a part of the Hemington Terrace unit at Lockington. These three images highlight the varying response of LiDAR intensity to geomorphological features.

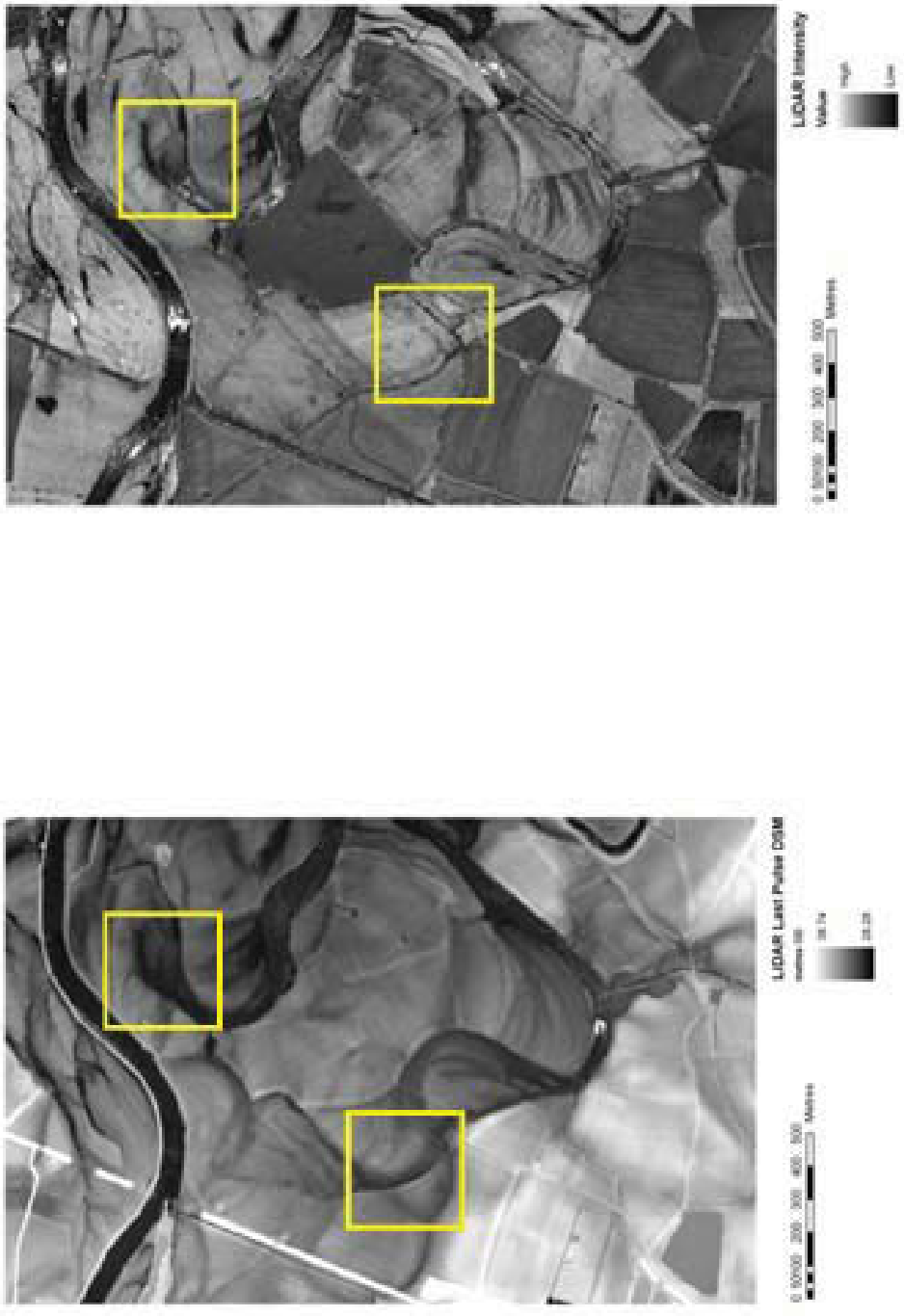

Fig 3.20: LiDAR elevation (bottom) and Intensity (Top) data for the Lockington study area. The yellow boxes highlight variations of the intensity response over palaeochannels of similar topographical character. That at the northern edge of the image produces a clear low intensity response, while that to the south is not reflected in the intensity data.

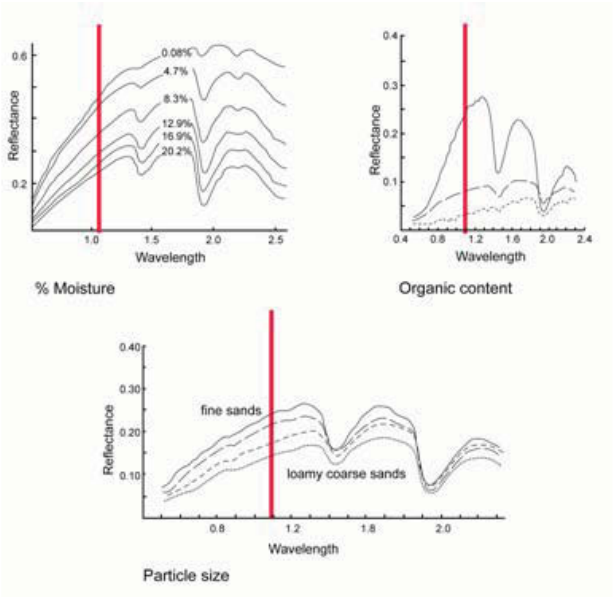

Fig 3.21: Graph showing the measured reflectance of sediments of differing moisture organic content and particle size across the spectrum. The NIR response (1047nm) is highlighted in red.

3.10.2 Aims and Objectives

The present work aimed to investigate the relationship between LiDAR backscatter laser intensity and soil and sediment properties:

- To investigate the relationship between topsoil moisture and laser intensity broadly across the study area to determine whether clearly an identifiable relationship exists between these two that holds true for different sediment types.

- To investigate in detail the relationship between topsoil moisture, laser intensity and topsoil organic content at three locations reflecting different geomorphological units across the site.

3.10.3 Method Statement

3.10.3.1 Toposil Moisture and Intensity: Broad Area Survey

Topsoil moisture was recorded at 29 locations across the study area (Fig. 3.22) using a Delta T Devices theta probe. Sample locations were chosen deliberately to represent a variety of geomorphological and topographical settings, for which some contrast was apparent in the LiDAR intensity data. The theta probe calculates *in-situ* volumetric soil moisture, logging readings to an attached data recorder. The location of each soil moisture reading was recorded using carrier phase differential GPS. GPS co-ordinates were used within the project GIS to extract intensity values from the LiDAR data.

Intensity/soil moisture values for each location were then examined and graphed to produce scatter plots showing the data pairs. Scatter plots were produced to show all soil moisture and intensity values and to show intensity/moisture values grouped by sediment type and for spatially discrete groups.

In addition a number of permanent sample locations were established for monitoring soil moisture through the soil profile to a depth of c 1m. Hand augered holes were lined with proprietary plastic sheaths to allow insertion of a Delta T Devices profile probe, which allow logging of soil moisture at 0.2m intervals on a 1.0m column. In the event the present of dense gravely sub-soil close to the surface made the placement of permanent sample locations all but impossible. In addition the tendency of the sheath lined holes to fill with water rendered measurements of soil moisture untenable. In the event this part of the field methodology was curtailed in favour of more intensive examination of the relationship between intensity and sediment character at selected key locations.

3.10.3.2 Topsoil Moisture, Organic Content and Intensity: Detailed Study

Detailed studies of topsoil moisture and organic content were undertaken at three discrete locations across the study site on the modern floodplain (Fig. 3.23: MF), the Hemington Terrace (Fig. 3.23: FF) and the Hemington Terrace edge overlapping with a palaeochannel (Fig. 3.23: MTF). At each location topsoil moisture readings were recorded at 4m intervals within a regular grid using a theta probe (Fig. 3.24). Topsoil samples were recovered from each sample location for subsequent laboratory analysis (Fig. 3.25). Each sample location was recorded using carrier phase GPS and the coordinates of the sample locations used to extract intensity values from the LiDAR data within the project GIS. Intensity/moisture/organic content data for each sample location were used to produce scatter plots for variable pairs. In addition, discrete moisture and organic content values were interpolated to produce a continuous grid representing variations in these variables to allow visual comparison with the LiDAR intensity data.

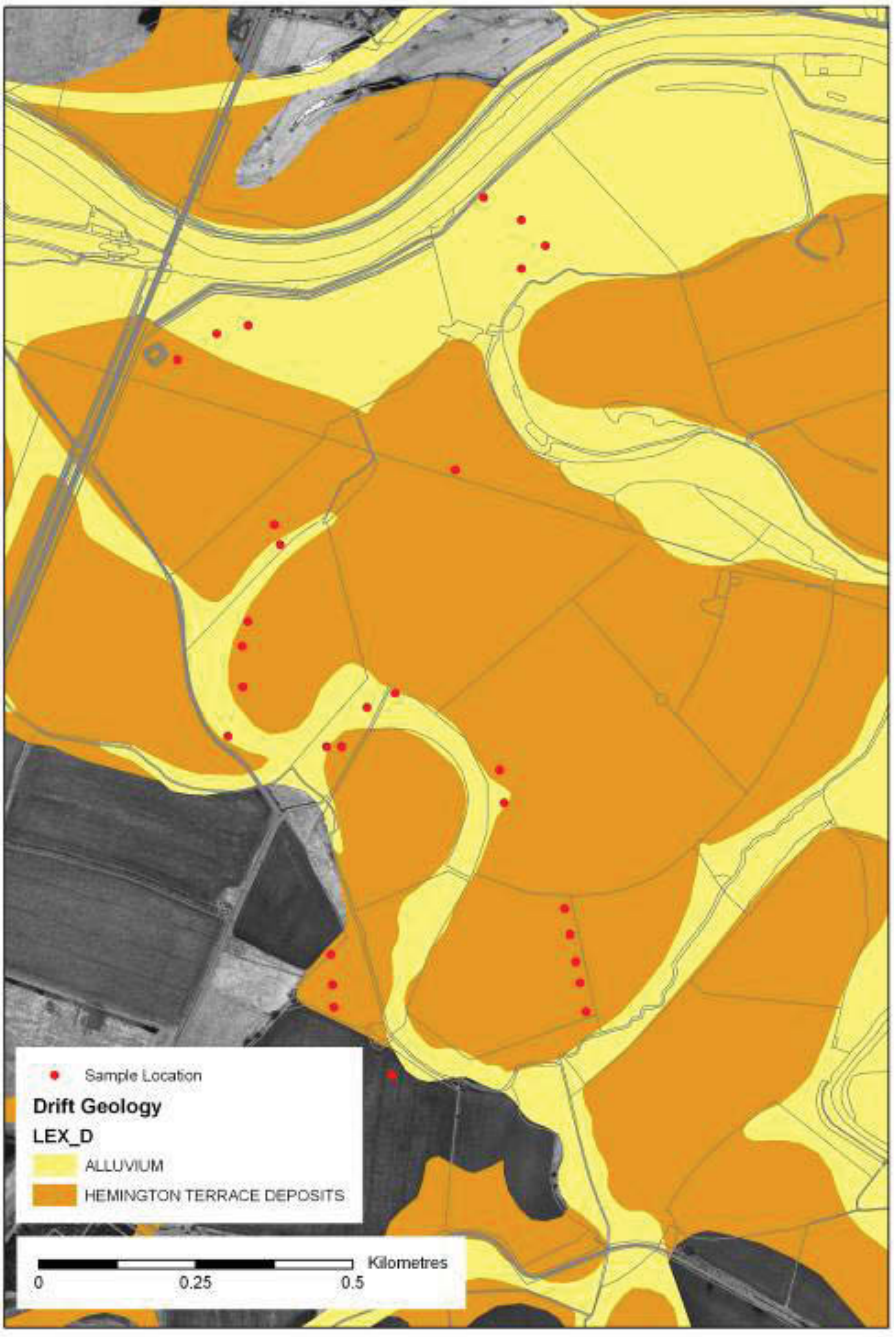

Fig 3.22: Sample locations for soil moisture/intensity comparison.

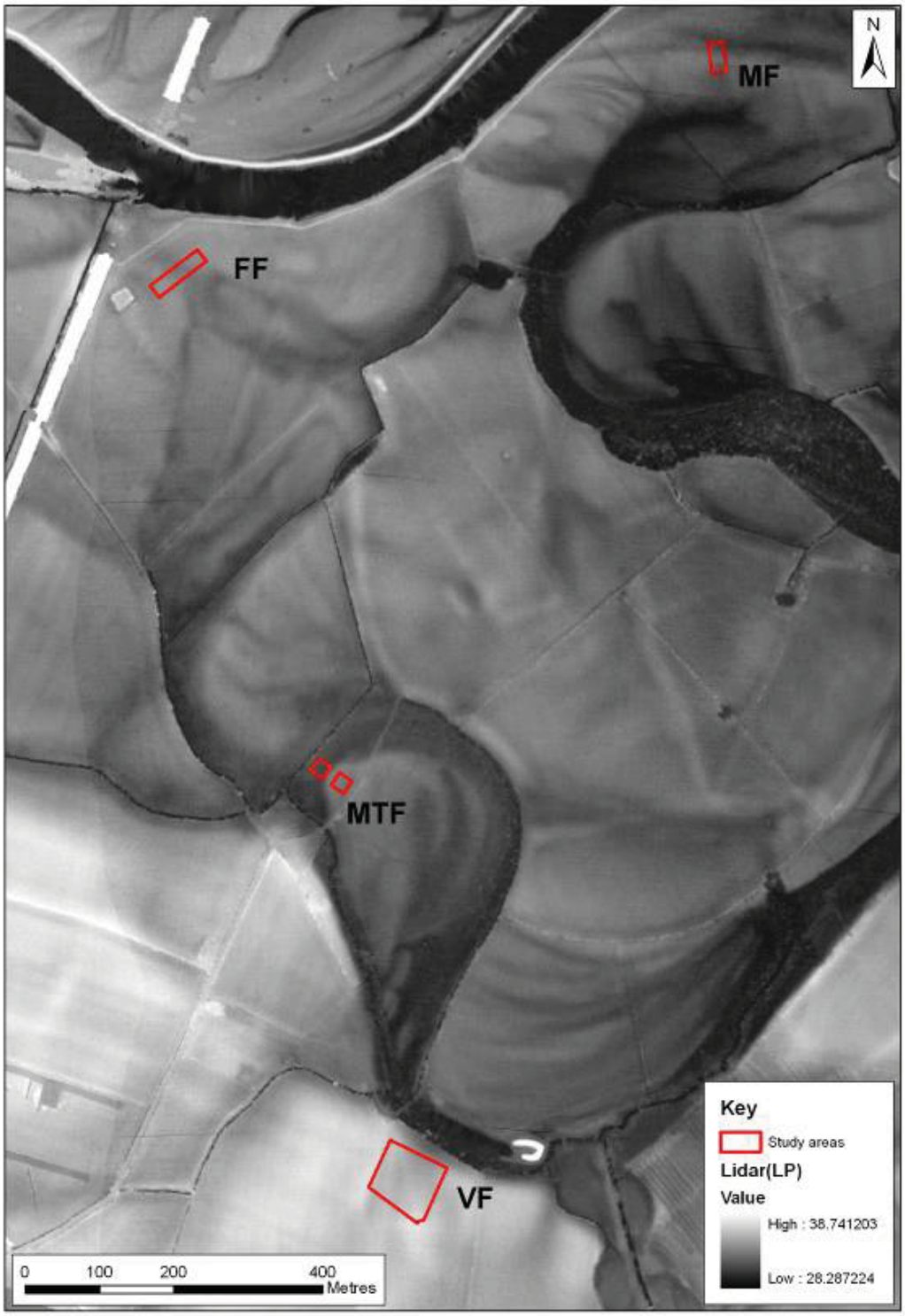

Fig 3.23: Lockington study area. LiDAR LPG elevation data with detailed LiDAR intensity study areas highlighted in red.

Fig 3.24: Lockington. Field collection of volumetric soil moisture data at regular grid intervals using a Delta T Devices Theta Probe.

Fig 3.25: Lockington. Field collection sediment samples for organic content analysis.

3.11 Data archive and query

ArcGIS provided the primary database for the project. ArcGIS is a Geographical Information System (GIS), which is used for the storage and exploration of data, linking together aspects of geomorphology and archaeology, in spatial and chronological dimensions. The investigation of an area of cultural landscape requires the collection of data from a range of sources involving both field based and desk based research. These strands of information are then placed together within a GIS, allowing relationships between variables to be visualised and explored.

A GIS is a spatially referenced database. Each variable can have a large number of attributes (categories) stored with it, giving a description of that variable. Data can be stored either as point data (e.g. an archaeological site), line data (e.g. a river) or as a vector (e.g. an area of river terrace). These data can then displayed and queried as a series of layers.

The following data were entered into the ArcGIS database:

I) Geomorphological maps, which were adapted through on screen digitisation
II) Geology maps supplied through the BGS
III) LiDAR intensity, DSM and DTM models
IV) IFSAR DSM and DTM models
V) Co-ordinates of the fieldwork survey areas
VI) GPR transect locations
VII) ER transect locations
VIII) Gouge core locations
IX) Palaeoenvironmental sample locations
X) OSL sample locations
XI) 1:10000 OS maps
XII) Digitised SMR data
XIII) Bore hole locations
XIV) Rectified aerial photographs of the study area

ArcGIS provided the primary means of integrating the various data sources. ArcScene was also employed to allow the layering of data in a quasi-3D environment, permitting direct visual comparison between the data types.

3.12 Ground penetrating radar materials and methods

The project also utilised GPR as a ground based prospection tool, which can be effective for the investigation of sub-surface sediment stratigraphy of alluvial depositional environments (e.g. Heinz and Aigner, 2003). The surveys used a 200MHz antenna frequency, with a GSSI SIR3000 unit, collecting data with distance calibration through a survey wheel. Data was collected using 512 samples/scan, with 16 bits per sample at 64 scans per second. Field filters were set at three times the antenna frequency for the IIR vertical high pass (600MHz) and one quarter of the antenna frequency for the IIR low pass (50MHz). On site calibration of the signal amplification was made on terrace gravels.

Within a floodplain context, boundaries between geomorphological units are seen as discontinuities, due to different sediment properties. The identification of radar terminations allows a relative chronology for a sequence of sediment units to be constructed (Bristow *et al.* 2005). Interfaces between different geomorphological units represent terminal events in either deposition or erosion (erosional bounding surfaces), and the start of subsequent processes (such as palaeochannel infilling). Estimating the depth of discontinuities within floodplain sediments is complex, due to different dielectric constants found within different geomorphological units. The electrical properties of a sediment unit effect the travel time for a radar pulse.

Within an alluvial context the relative dielectric permittivity (RDP) of different sediment units is critical (the ability of sediment to absorb, reflect and be permeated by, the radar pulse). To calibrate the electric depth model created by the GPR the dielectric properties of the soil profile need to be accurately estimated. Within alluvial environments this is difficult as any GPR transect is likely to cross a series of contrasting geomorphological units, each having a different RDP. Within this project the dielectric constant of the soil was calibrated through comparison with gouge core transects drilled by the project team (Bridge *at al.* 1998). The gouge core transects allowed the depth of silty clay alluvium overlying the gravels to be accurately measured. Gouge core sampling was undertaken at 10m intervals along specific GPR transects. The depth of each sediment unit was recorded with a description of its composition before impenetrable gravel was encountered. All GPR surveys were set out and recorded using differential GPS.

The GPR data was processed through setting the correct time zero and correcting for hyperbola reflections via migration. Background removal filters, vertical high pass and vertical low pass filters were used to process the data. This is a simple processing sequence that produces good quality results in alluvial data sets. ArcGIS (© ESRI, version 8.3) was used to co-register, integrate and query the data. LiDAR data was imported as point cloud data and transformed into a TIFF image within ArcGIS. The GPR data was processed in Radan (© GSSI, version 6.0) and depth slices were exported as XYZ data. Images were produced within Surfer (© Golden software INC, version 8.02) and imported into ArcGIS as TIFF images files. The HER data was imported as point data with recorded attributes such as site name, method of identification, archaeological interventions or archaeological period, and was provided by Leicestershire and Derbyshire County Councils. Aerial photographs were imported as JPEG georectified images. The geomorphological and chronostratigraphic models were produced through the on-screen digitisation of 1:5000 field maps, using attribute encoded polygon shape files. Geological information was supplied by BGS as polygon shape files mapped at 1:50,000, with solid and drift geologies. The pseudo 3D modelling was undertaken in ArcScene (© ESRI, version 8.3).